

https://dspace.org/

Noise and interference reduction in amplitude modulation

Borochov, Amos

2016-08-17
http://hdl.handle.net/10539/20877

Downloaded from a DSpace repository. https://dspace.org/

Lets multiply $V_m(t)$ with the sinusoidal carrier signal, $V_c(t)$, where

$$V_c(t) = A_c \cos\omega_c t = A_c \cos 2\pi f_c t$$

$$= \frac{A_c}{2} \left(e^{j\omega_c t} + e^{-j\omega_c t}\right) = \frac{A_c}{2} \left(e^{j2\pi f_c t} + e^{-j2\pi f_c t}\right) \qquad (2.1\text{-}2)$$

A_c is the amplitude of the carrier signal
f_c is the frequency of the carrier signal

By using the identity:

$$\cos\alpha \cos\beta = \tfrac{1}{2} \cos(\alpha + \beta) + \tfrac{1}{2} \cos(\alpha - \beta)$$

the product of $V_m(t)$ and $V_c(t)$ is:

$$V_m(t)\ V_c(t) = \frac{A_m A_c}{2} \left[\cos(\omega_c + \omega_m)\, t + \cos(\omega_c - \omega_m)\, t\right]$$

$$= \frac{A_m A_c}{4} \left(e^{j(\omega_c + \omega_m)t} + e^{-j(\omega_c + \omega_m)t} + e^{j(\omega_c - \omega_m)t} + e^{-j(\omega_c - \omega_m)t}\right) \qquad (2.1\text{-}3)$$

the new signal occupies the range $2f_m$, from $f_c - f_m$ to $f_c + f_m$ and is called "baseband" which is the signal bandwidth.

The frequency range f_c to $f_c - f_m$ is called lower sideband, while f_c to $f_c + f_m$ is called upper sideband.

2. BACKGROUND

This chapter describes the existing methods for generation and detection of amplitude modulated signals. The performance of the various detectors were carefully evaluated since their limitations gives the motivation for this work. The chapter concludes with literature survey of interference rejection in modern receivers.

2.1 AM GENERATION

One of the goals in communication engineering, is to design a system which allows many stations to be transmitted simultaneously over a single communication medium - the electromagnetic spectrum. The method which allows to do so called "multiplexing". By shifting each station to different frequency band we get "frequency multiplexing". The individual stations can be separated by filtering. Frequency multiplexing makes use of an auxiliary waveform called a carrier. When the carrier is multiplied with the station message we get amplitude-modulation waveform. (Bell Telephone Laboratories 1964).

Lets assume that the signal, $V_m(t)$, is a sine waveform given by:

$$V_m(t) = A_m \cos\omega_m t = A_m \cos 2\pi f_m t$$

$$= \frac{A_m}{2}\left(e^{j\omega_m t} + e^{-j\omega_m t}\right) = \frac{A_m}{2}\left(e^{j2\pi f_m t} + e^{-j2\pi f_m t}\right) \qquad (2.1\text{-}1)$$

A_m is the amplitude of the signal

$f_m = \frac{W_m}{2\pi}$ is the frequency of the signal

The remainder of this document will describe the existing techniques and their limitations, literature survey of interference rejection in modern receivers, design and theoretical analyses of the new detector and test results.

Chapter 2 will describe the conventional methods for generation and detection of amplitude modulated signals, their limitations and modern techniques for interference rejection.

Chapter 3 deals with the design of the new detector. Its practical design considerations is closely matched to its theoretical analysis. The attached circuit diagram is given in order to allow full understanding down to component level.

Chapter 4 gives the results of the comprehensive test conducted on the new detector. All tests are documented, plotted and tabulated. In addition an audio cassette is attached to this report in order to further illustrate the results.

Chapter 5 concludes the work and gives recommendations for improvements that could not be implemented due to time restrictions.

1. INTRODUCTION

The purpose of this project, is to develop, construct, and test an AM detection technique for radio signals with improved performance to conventional detection, when operating in a non optimum condition. (Shannon, C.E. 1949 : p10-21).

AM modulation is widely used and any improvement in performance, especially in noisy HF channel, will contribute to better communication.

The new detector should out-perform the conventional detectors in three points:

1) The signal to noise ratio at the output will be higher than at the input, which is impossible in conventional AM detection. (Davenport, W. and Root, W. 1958).

2) Reduce interference which appears at one sideband only.

3) Lower threshold of detection.
(Taub, H. and Schilling, D.L. 1971 : p83-88).
Threshold - the point chosen arbitrarily at which the output signal to noise ratio falls away by 1 dB from the input signal to noise ratio.

On the other hand the new detector will not function properly under the following conditions:

1) Interfering signal with level higher than the wanted carrier of the signal and frequency close to the wanted carrier.

2) Interfering signals at both sidebands and at approximately the same distance from the carrier.

CONTENTS (CONTD.)

FIGURES

FIGURE 2.1 : ENVELOPE DETECTOR 6

FIGURE 3.1 : BLOCK DIAGRAM 18

FIGURE 3.2 : OUTPUT VERSUS INTERFERENCE 31

APPENDICES

APPENDIX A: TEST RESULT PLOTS

APPENDIX B: SQUARE-LAW DEMODULATOR

APPENDIX C: ENVELOPE DEMODULATOR

APPENDIX D: CIRCUIT DESCRIPTION

APPENDIX E: CIRCUIT DIAGRAM

APPENDIX F: RECORDING

REFERENCES

.oOo.

CONTENTS (CONTD.)

PAGE

3. DESIGN AND IMPLEMENTATION 16

3.1 IMPROVEMENTS 16

3.1.1 General Description of the New Detector 17

3.2 DETAIL DESIGN CONSIDERATION 19

3.2.1 PLL 19

3.2.2 Multipliers 20

3.2.3 A to D Conversion 21

3.2.4 FFT 21

3.2.5 Expandor 24

3.2.6 Final Conversions 25

3.3 THEORETICAL ANALYSIS OF THE NEW DETECTOR 25

3.3.1 FFT Resolution 25

3.3.2 White Noise Reduction 26

3.3.3 Sideband Selection 28

3.3.4 Problem Due to Sideband Selection . . . 30

4. RESULTS 32

4.1 PRELIMINARY 32

4.2 RF SIMULATION TESTS 34

4.3 ANALYSIS 42

4.4 RECEIVER SENSITIVITY TEST 51

4.5 LISTENING TEST 53

5. CONCLUSIONS 55

5.1 SUMMARY OF WORK 55

5.2 SUMMARY OF RESULTS 55

5.3 CONCLUSION 57

5.4 RECOMMENDATIONS FOR IMPROVEMENT 57

CONTENTS

PAGE

DECLARATION i

DEDICATION ii

ABSTRACT iii

ACKNOWLEDGEMENTS iv

CONTENTS v

1. INTRODUCTION 1

2. BACKGROUND 3

2.1 AM GENERATION 3

2.2 AM DEMODULATION 5

2.3 AM WITH NOISE 7

2.4 SIGNAL TO NOISE RATIO 8

2.5 SQUARE-LAW DEMODULATOR 10

2.6 ENVELOPE DEMODULATOR 10

2.7 CONCLUSION 11

2.8 INTERFERENCE REJECTION IN MODERN RECEIVERS LITERATURE SURVEY 12

2.8.1 Passband Tuning 12

2.8.2 IF Notch Filter 13

2.8.3 Audio Notch Filter 13

2.8.4 RF Noise Blanker 14

2.8.5 Audio Noise Blanker 14

2.8.6 Filter Bank 14

2.8.7 Impulse Noise 15

ACKNOWLEDGEMENTS

Tellumat Electronic Components

GEC Plessey Semiconductors

Alcatel Altech Telecoms

Allied Electronic Components

Analog Devices

Burt Gildenhuys

ABSTRACT

Amplitude modulation, is the oldest modulation technique used for voice communication. It is the simplest and cheapest way to modulate and demodulate voice, and as a result, it did not lose much popularity in spite of the development of other, more efficient modulation technique. This project offers a new approach for AM demodulation.

The two sidebands are separated and divided into many sub-bands. The signals with the lowest noise level are selected and their levels are individually adjusted according to signal conditions.

The result is reduction of over 35 dB in continuous interference and about 15 dB in white noise level.

The new detector out-performs the conventional detectors in all aspects and can be used in applications where top performance is required and where money is no object.

DEDICATION

To my beloved wife Angie for her continual support and encouragement, and to my dear son Rafi.

DECLARATION

I, Amos Borochov, declare that this project report is my own unaided work. It is being submitted for the Degree of Master of Sciences in Engineering in the University of the Witwatersrand, Johannesburg. It has not been submitted before for any degree or examination in any other University.



AMOS BOROCHOV

10th day of March 1995

NOISE AND INTERFERENCE REDUCTION IN AMPLITUDE MODULATION

by: AMOS BOROCHOV

A project report submitted to the Faculty of Engineering, University of the Witwatersrand, Johannesburg, in partial fulfilment of the requirements for the degree of Master of Science in Engineering.

Sandton, 1995.

3. DESIGN AND IMPLEMENTATION

This chapter describes the design of the new detector and the way it was implemented in a practical circuit. Theoretical analysis, which was part of the design process, is presented in order to allow comparison between the calculated and the measured results in tne following chapter.

3.1 IMPROVEMENTS

It was shown in Chapter 2 that the synchronous demodulator gives the best performance. The new design will attempt to improve its performance in two main areas:

1) The synchronous demodulator produces output signal to noise ratio, equal to the input signal to noise ratio. The new detector should have higher signal to noise ratio at the output than at the input (reduction of white noise level). (Hawkins and Stevens 1950))

2) In the synchronous demodulation, interference at one sideband appears at the output as signal, decreasing intelligibility and causing masking effect. (Bos and De Boer, J. 1966). (Masking effect is psychoacoustic phenomena, in which strong signals mask weak signals and make them inaudible).

   The new detector should reject strong interference appearing at one sideband only, and thus reducing the effect (reduction of continuous interference).

The signal power in each filter is measured and filters with output substantially above the mean level are switched out. It should be pointed out that their method is doing similar functions and opposite functions to the detector designed in this work. The similar function is selecting the lower amplitude bands as is done in the sideband selection mode.

The opposite function is the noise reduction which attenuates low level signals and noise as opposed to the suggested circuit which passes low level signals and cuts high level noise.

2.8.7 IMPULSE NOISE

According to (Sabin, W.E. and Schoenike, E.O. 1987), impulse noise differs from ordinary random noise in two respects. Its short term spectrum is phase coherent, and has an amplitude variation and autocorrelation, as a result, the received voltage is nearly proportional to bandwidth rather than to the square root of bandwidth. Since the pulse power is very high for a short time and then falls quickly to zero, it is sufficiently different from speech and the receiver noise blanker can detect it. Speech can be interrupted for about 10 percent of the time with an acceptable loss of articulation.

The problem is solved in the synchronised detector as long as a good phase lock loop is utilised. If this is the case, the audio notch filter can work well.

2.8.4 RF NOISE BLANKER

RF noise blanker (Dawson, S.L. 1984) detect wideband high amplitude interference and cut the signal pass for a short time. It must be placed before the IF filters in order not to allow the filters time constant to stretch the pulse.

2.8.5 AUDIO NOISE BLANKER

Audio noise blanker (The American Radio Relay League 1992), works in a similar way to the RF one. It has a few ms delay time before the switch, and track and hold circuit after the switch. The advantages are that the pulse detector has time to detect the pulse, and open the audio switch before the pulse reaches the switch, the track and hold fills the gap created by opening the switch with the last signal level, and eliminating the hole in the audio. The disadvantages are, that the pulse will be stretched in the IF filters, long pulse will effect AGC generation and reduce signal level, and narrow high amplitude pulses can cause ringing in the IF filters and saturation in the amplifiers, which result in recovery time much longer than the pulse itself.

2.8.6 FILTER BANK

A filter bank is suggested in (Maslin, N.M. 1987). According to this method the signal and the interference are passed through a bank of identical filters which cover the total signal bandwidth. Each filter has a bandwidth of less than 100 Hz.

2.8.2 IF NOTCH FILTER

IF notch filters (The American Radio Relay League 1992) allow creation of a notch in the passband, in order to reject interference from a stable frequency source, that beat with the carrier. It can be very effective against carriers from other AM stations and CW transmissions. Since the filter operates at IF frequency, the bandwidth is fairly high, but in AM because of the presence of two sidebands, all it means is reduction of max. 3 dB in audio level. The IF notch filter is in most cases, inserted before the AGC detection. The advantage is that the interfering signal does not interfere with AGC level, and the station is received with constant amplitude. The disadvantage is that if the interference is strong enough, it will saturate the IF stages which will result in intermodulation distortion.

2.8.3 AUDIO NOTCH FILTER

An audio notch filter (The American Radio Relay League 1992) operates at audio frequency, and is placed after the demodulation. Its bandwidth is narrow, and it creates a hole in the spectrum. It can be coupled to a phase lock loop in order to track the interference automatically. It has some advantages and some disadvantages comparing to IF notch filter. In SSB reception, it will have less effect on audio quality because of the narrow bandwidth of the notch. In AM reception, on the other hand, it will work well, as long as the interference is weaker than the carrier. Strong interfering signals will cause the common envelope demodulation to demodulate the sidebands with respect to the interference and not the carrier.

2) The noise spectrum extends up to half the IF bandwidth, while in the other detection noise at one edge of the IF passband demodulates against noise at the other edge, thus producing audio noise extending up to the full IF bandwidth.

3) Selective fading can attenuate the carrier by over 20 dB. (CCIR 1974 Rec. 339-3). When this happens, the envelope and the square-law demodulator will produce very high levels of distortion since the input will look like an over-modulated signal. The synchronous demodulator will not suffer from this problem, since the carrier is produced internally by the local oscillator.

(Law H.B. 1957).

2.8 INTERFERENCE REJECTION IN MODERN RECEIVERS LITERATURE SURVEY

2.8.1 PASSBAND TUNING

New receivers include various circuits to improve their interference rejection. Passband tuning (The American Radio Relay League 1992) allows the user to independently reduce the IF bandwidth at the upper and lower ends in order to reduce co-channel interference. In AM reception the use of this circuit is limited to one sideband only, since the bandwidth reduction of both sidebands will effect the audio high frequency response.

2.7 CONCLUSION

If the signal to noise ratio is >10dB which is the minimum ratio for voice communication (Fletcher, H. 1953), all three detectors will give about the same performance, but as the signal to noise ratio becomes smaller. The envelope demodulator has a threshold at about $\frac{P_c}{N_m}$ = 6 dB, the square-law demodulator at about $\frac{P_c}{N_m}$ = 4,6 dB, but the synchronous demodulator has no threshold limits at all.

(Taub, H. and Schilling, D.L. 1971 : .0).

So far it was assumed that only white noise is present at the input to the demodulator (Kryter, K.D. 1962 : p1689-1697). In practice this situation will only occur at VHF frequencies and above. (Evans, D.S. and Jessop, G.R. 1976). At HF the noise will mainly be, interference from other stations (Maslin, N.M. 1987 : p92), static (CCIR 1974 Report 322-1) and fading due to poor reflection. (Budden, K.G. 1985). At MW and LW the noise will mainly be static and man made. (CCIR 1978 Report 258-3). It is obvious from the above that the synchronous demodulator has advantages far beyond the absence of threshold, as was demonstrated in the white noise case.

In practice it will give the following advantages: (Electronics and Wireless World September 1989 : p858).

1) Lower noise level, since noise in quadrature is rejected.

2.5 SQUARE-LAW DEMODULATOR

The square-law demodulator behaves differently (see Appendix B) and its output signal to noise ratio is:

$$\frac{S_o}{N_o} = \overline{m^2(t)}\ \frac{P_c}{N_m}\ \frac{1}{1 + 3/4\,(N_m/P_c)} \qquad (2.5\text{-}1)$$

The term $\frac{1}{1 + 3/4\,(N_m/P_c)}$ gives the threshold effect. When the carrier power P_c is much larger than N_m, this term can be ignored, but for low signal to noise ratios, it will have an increasing effect.

(Taub, H. and Schilling, D.L. 1971: p290).

2.6 ENVELOPE DEMODULATOR

The envelope demodulator has similar characteristics, (see Appendix C), and when the signal to noise ratio is low its output will be:

$$\frac{S_o}{N_o} = \frac{\overline{m^2(t)}}{1.1}\left(\frac{S_i}{N_m}\right)^2 \qquad (2.6\text{-}1)$$

(Taub, H. and Schilling, D.L. 1971: p290).

Let the received signal be:

$$S_i(t) = A[1 + m(t)] \cos 2\pi f_c t$$

$$= A \cos 2\pi f_c t + Am(t) \cos 2\pi f_c t \qquad (2.4\text{-}1)$$

the term $\overline{m^2(t)}$ is the time average of the square of the modulating waveform

if the modulation is sinusoidal

$$\overline{m^2(t)} = \frac{m^2}{2}$$

and

$$\frac{S_o}{N_o} = \frac{m^2}{2+m^2} \frac{S_i}{\eta f_m}$$

(2.4-2)

The term $\frac{m^2}{2 + m^2}$ is the figure of merit for sinusoidal modulation in AM system defined by $\gamma = \frac{S_0/N_0}{S_i/N_i}$ (2.4-3)

(Taub, H. and Schilling, D.L. 1971 : p281)

as can be seen, in synchronous demodulation the output signal to noise ratio is closely following the input signal to noise ratio without threshold.

(Threshold : a point at which the output signal to noise ratio falls away by 1 dB from the input signal to noise ratio).

(Viterbi, A.J. 1966).

(In practice the phase-locked-loop that locks on the carrier has its own threshold).

(Blanchard, A. 1976)

$S_i^{(SB)}$ is the power in the sideband.

S_o is the output signal power.

N_o is the output noise power.

f_m is the bandwidth.

η is the spectral density
where the noise is gaussian, white and of two-sided power spectral density $\eta/2$, since the noise spectral power density $G_n(f) = \eta/2 = P/2B$
P is the noise power present at the demodulator input in the bandwidth B.

S_o/N_o serves as a figure of merit of the performance of a communication system.

2.4 SIGNAL TO NOISE RATIO

In order to increase the output signal to noise ratio one can take the following steps:

1) Increase the signal power by using stronger transmitter and higher gain antennas.
2) Restrict the baseband frequency range, 200 Hz to 3000 Hz for communication quality audio.
3) Make the receiver and the communication channel quieter.

(Sakrison, D. 1968).

After dropping dc terms and terms located near ω_c and $2\omega_c$ by using low-pass filter, the output is:

$$S_o(t) = kA_c^2[m(t) + \tfrac{1}{4} m^2(t)] \qquad (2.2\text{-}4)$$

The term $m^2(t)$ is distortion but this has no significance since

$$\tfrac{1}{4} m^2(t) << |m(t)| .$$

(Taub, H. and Schilling, D.L. 1971 : p94)

2.3 AM WITH NOISE

So far, a very important fact was neglected, that in any real system, when the signal voltage arrives at the demodulation, it will be accompanied by a voltage waveform which varies with time in an entirely unpredictable manner.

This unpredictable voltage waveform is a random process called noise.

(Davenport, W. and Root, W. 1958).

Let's consider the case that synchronous demodulator detects the AM signal. The carrier is used as a transmitted reference to obtain the reference signal cos $\omega_c t$. The carrier increases the total input signal power but makes no contribution to the output signal power.

(Taub, H. and Schilling, D.L. 1971 : Pg.281)

$$\frac{S_o}{N_o} = \frac{S_i^{(sm)}}{\eta f_m} \qquad (2.3\text{-}1)$$

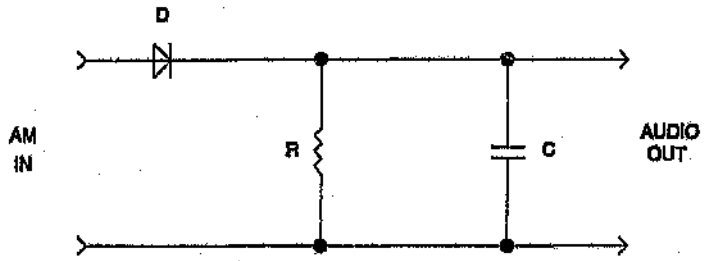


FIGURE 2.1 : ENVELOPE DETECTOR

the diode is charging the capacitor to the peak value of the incoming signal, and the resistor is discharging the cap. Since the RC time constant is short compared to the audio frequency, but long compared to the carrier frequency, the output will follow the carrier envelope.

(Roddy, D. and Coolen, J. 1981 : p266).

The third method for detection of AM signal, is the square-law demodulator. Such demodulation is carried out by passing the AM signal through a non-linear device. If we assume that the device has a square-law relationship between input signal x and output signal y.

$y = kx^2$ $\qquad\qquad$ k = constant

Because of the non-linearity, the output is different from positive and negative swings of the carrier away from the quiescent operating point 0 of the device. If the input signal is:

$$x = A_c + A_c\,[1 + m(t)]\,\cos\,\omega_c t \qquad (2.2\text{-}2)$$

A_0 is the amplitude of quiescent operating point the output is:

$$y = k(A_c + A_c\,[1 + m(t)]\,\cos\,\omega_c t)^2 \qquad (2.2\text{-}3)$$

2.2 AM DEMODULATION

The recovery of the baseband signal is simple. Let a signal $m(t)$ be band limited to the frequency range 0 to f_m and translated out of its baseband through multiplication with cos $\omega_c t$, the recovery will take place by multiplying again with $\omega_c t$.

$$[m(t) \cos \omega_c t] \cos \omega_c t = m(t) \cos^2 \omega_c t$$
$$= m(t) (\tfrac{1}{2} + \tfrac{1}{2} \cos 2 \omega_c t)$$
$$= \frac{m(t)}{2} + \frac{m(t)}{2} \cos \omega_c t \qquad (2.2\text{-}1)$$

(Taub, H and Schilling, D.L. 1971 : p83-88)

Since $f_c >> f_M$ the double frequency term is removed by a low-pass filter, this operation is called synchronous or coherent detection.

(Tucker, D.G. 1954 : p143).

The most common way to demodulate an AM signal is the envelope demodulator.

(Macario, R.V.C., Craine, J.F. and Walters, D.S. 1974 p101-108).

3.3.3 SIDEBAND SELECTION

The effect of the sideband selection will benefit reception on short wave where co-channel interference can be an important factor (Dutta, S. and Gott, G.F. 1982). High level audio signal masks lower level signal at nearby frequencies. The degree and the spread of the masking, depends on the amplitude and spectral content of the audio band. Selecting the FFT bin with the lower amplitude will greatly improve interference rejection, unless of course both sidebands contain interference, with frequencies close enough to fit into the same bin in both FFT's. The ability of the detector to handle interference with high amplitude should also be analyzed since it is the function of the dynamic range of the individual stages. The double balanced modulators have third order interception points of -15 dBm (+5dBm output because of RF gain), noise figures of 5dB and in properly designed circuit can operate over 100 dB dynamic range (Philips, Linear Products, 1988). The switch capacitor filter (before the A to D converters) has total C message noise of 6 dBrncO (INTEL 1990) which gives -90 + 6 = -84 dB noise level. The 16 bits A to D converter has sample and hold noise of 115 μVrms when operating in 20 V bipolar mode as a result the noise floor will be :

$$20\ V_{BIPOLAR} = \frac{20}{2\sqrt{2}} = 7,07\ Vrms$$

$$N = 20 \log \frac{115x10^{-6}}{7,07} = -95,77\ dB$$

On the other hand if No. 8 is used ($\sqrt{x}$), the noise level will drop to -17 x 2 = -34 dB but the signal level will stay the same. After the reverse FFT the combined noise level will increase to -17 dB with no change in signal level (0 dB).

This operation will give 17 dB improvement in signal to noise ratio. It should be mentioned, that the improvement is a function of the input signal to noise ratio, and is independent of signal level, since the compressor located after the D to A converter, compensates for any change of level. This example, does not represent real life situation, in which more than one signal is present, and the signals fall between the bins.

As an example, lets assume that position No. 8 is used ($x^{1/N} = x^{\frac{1}{2}} = \sqrt{x}$) and three signals with levels of 1/2, 1/4, 1/8 are at the input (-6 dB, -12 dB, -18 dB respectively). After the expansion process the levels will be $(1/2)^2 = 1/4$, $(1/4)^2 = 1/16$, $(1/8) = 1/64$ (-12 dB, -24 dB, -36 dB respectively).

When the composite signal is passing through the compressor only the strongest signal will effect its gain cell and the first signal will become $(1/4)^{\frac{1}{2}} = 1/2$ (-6 dB). As can be seen the compressor, under the above conditions behaves as x2 amplifier. The second signal will be 1/16 x 2 = 1/8 (-18 dB) and the third signal will be 1/64 x 2 = 1/32 (-30 dB). It can be seen from the above example that the strongest signal stays at the same level, the second dropped by (-18 dB)-(-12 dB) = -6 dB and the weakest signal dropped by (-30 dB)-(-18 dB) = -12 dB.

bandwidth of each point is 31,25 x 1,81 = 56,56 Hz. Random impulse noise will tend to be averaged out but speech which has phrases with minimum length of 30-50 ms and continuous interference will pass.

In the presence of white noise the power spectral density of each point will be:

10 log (56,56/3200) = -17,53 dB below average noise level.
Another way to explain this operation is to think of the FFT as a band of equally spaced filters in which 102 of them are in the wanted bandwidth, their centre frequency is 31,25 Hz apart and their 6 dB bandwidth is 56,56 Hz. It should be noted that the filters are overlapping each other but for simplicity this point was ignored.

3.3.2 WHITE NOISE REDUCTION

The amount of white noise reduction depends on the switch setting of the noise threshold detector and the characteristic of the signal itself. If we take for example an extreme case in which we have a continuous sine wave with a magnitude equal to the noise level (0 dB) and a frequency in the middle of the bin. After the FFT the signal will stay at the same level, but the level of each point containing noise will drop to about -17 dB. If noise reduction No. 1 is used (no reduction) in the reverse FFT the noise level of the individual points will combine and the output will be identical to the input.

3.2.6 FINAL CONVERSIONS

The next stage is polar to cartesian converter, that converts the phase and the magnitude into real and imaginary components.

$R = M \cos \phi$
$I = M \sin \phi$

Reverse FFT is the last operation performed in DSP, and the output is fed into 16 bit digital to analog converter.

3.3 THEORETICAL ANALYSIS OF THE NEW DETECTOR

Due to the complex nature of the new detector, it is not practical to give a fixed calculated number to describe its performance, and the effect of each operation will be analyzed separately. The definition of noise should also be changed, from random signal (white noise) to any signal which is not the wanted signal.

The new detector will have all the advantages of very high performance synchronous demodulator, which gives threshold free detection down to at least -10 dB below noise level (limited by the phase lock loop).

3.3.1 FFT RESOLUTION

The FFT has 256 points. Since the sampling rate is 8 kHz, each point represents 8000/256 = 31,25 Hz bandwidth. The total audio bandwidth is 200 Hz to 3,4 kHz, 3400 - 200 = 3200 Hz, so the number of usable points is ≈102 points. Blackman-Harris window operator has 6 dB bandwidth of 1,81 thus the 6 dB

3.2.5 EXPANDOR

The next stage is the amplitude expandor stage. Short pulses of noise tend to be averaged out in the FFT, while long signals which are continuously comparing to time constant of the FFT (256 : 8000 Hz = 32 ms) will retain their original value. Since the amplitude of the signal and the noise vary continuously due to change in propagation condition, interference from other stations and AGC operation, it is impossible to use a fixed value expansion.

The solution was to use look up table with exponential curve. External switch with eight positions allows the user to select the amount of noise reduction needed according to signal condition. Position 1 is intended for good condition and all signals are allowed to pass without any change. The 8 switch positions give:

POSITION	
1	N = 1.000000000
2	N = 1.104089510
3	N = 1.219013696
4	N = 1.345900179
5	N = 1.485994269
6	N = 1.640670685
7	N = 1.811447293
8	N = 2.000000000

The output is $(x)^{\frac{1}{N}}$, where x = input magnitude. The higher positions are intended to be used in extreme conditions only, since they will degrade audio quality. (More information about the amplitude expandor is given in Chapter 3.3).

It should be noted, that in order to meet the design goal of proper operation when the interfering signals are stronger than the wanted signal by +10 dB, the wanted signal must be set at 14 bit level in order to provide 2 bit headroom (12 dB), thus putting more demands on the dynamic range of the FFT.

The real and imaginary outputs of the FFT's are crossed and then added and subtracted from each other in order to produce the upper and lower sidebands. (In order to produce one side band, the real component of the 0^0 signal is added to the imaginary component of the 90^0 signal and the imaginary component of the 0^0 signal is added to the real component of the 90^0 signal. The second side band is produced in a similar operation but instead of adding the signals the 90^0 components are subtracted from the 0^0 components). The signals are then converted to polar form by pythagoras processor.

Let R = real
I = imaginary
M = magnitude
Ø = phase

$$M = \sqrt{R^2 + I^2}$$

$$\text{Ø} = \text{arc tan } \frac{I}{R}$$

The two sidebands magnitude are then compared in a magnitude comparator, and the sideband with the lowest magnitude, is selected to pass on.

A common rule of thumb, defines the resolution of an FFT system as half the full width of the mainlobe. The width of the mainlobe for the Blackman-Harris window is six bins (points). The performance obtained from this window are:

Highest side lobe	-67 dB	
Mid-point loss	1,13 dB	
Overall loss	3,45 dB	
6 dB Bandwidth	1,81	(Harris, F.J. 1978)

Data precision of the FFT is a very important factor, since the new detector must be able to handle interference 10 dB above the signal. During each pass of a radix-4 FFT, it is possible for a particular result to grow by a factor of up to four in the first pass, and 5,242 in subsequent passes. This is between two and three bits in each pass, and the data path must allow for this word growth to avoid any possibility of overflow. If at the end of each data pass the word is reduced to 16 bits, by discarding the least significant bits to prevent overflow, the result is loss of arithmetic precision and poor dynamic range. This situation will become worse when the incoming data does not fully occupy all the bits in the word. The problem is overcome by using block floating point, which compensates for any unnecessary word growth.

During each pass the number of sign bits in the largest result is recorded. Before the next pass, data is shifted left (multiplied by 2), once for every extra sign bit in this recorded sample. At least one component in the block then fully occupies the 16 bit word, and maximum data accuracy is preserved. More detail about the FFT operation is in

(Plessey Semiconductors 1990c).

3.2.3 A TO D CONVERSION

The analog to digital converter operates at 8 kHz which is sufficiently fast, (more than twice the signal frequency to avoid aliasing), since the input is limited to 3,4 kHz, they produce 16 bit output and have external gain and offset adjustments.

(Analog Devices 1989/90).

3.2.4 FFT

The two signals, the in-phase and the quadrature are then fed to radix-4 256 points (Ref 37) FFT process. Since the sampling rate is 8 kHz each point represents 8000/256 = 31,25 Hz bandwidth (plus the window). The total audio bandwidth is 200 Hz to 3,4 kHz, 3400 - 200 = 3200 Hz, so the number of useable frequency points is:

$$\frac{3200}{8000} \times 256 = 102.4 \approx 102 \text{ points}$$

Blackman-Harris (3 term) operator window was chosen in order to increase the performance of the FFT.

It takes the form:

$$A - B\cos x + C\cos 2x$$

$$\text{where } x = \frac{2\pi n}{N}$$

$$n = 0 \text{ to } N-1$$

A = 0,42323, B = 0,49755, C = 0,07922

frequency stability (slow change in frequency, normally caused by temperature variation and poor design) on transmission, and spurious phase (unwanted AM to PM conversion, usually due to non-linearities in IF stages and especially the limiter stage before the phase detector) modulation by the wanted audio. The loop should not attempt to follow the rapid polarity inversion of a carrier, which has experienced a selective fading and has flywheeling action (the ability of the PLL to stay locked during short intervals in which the signal either disappears or was covered with noise), during lightning storms. In order to meet all the above contradicting requirements, external controls were provided in order to adapt to varying signal conditions. The PLL has four positions for loop bandwidth: 250 Hz, 80 Hz, 40 Hz, and 20 Hz. The AGC nas three positions for loop bandwidth: 80 Hz, 40 Hz and 20 Hz.

(Best, Dr. R.E. 1978).

3.2.2 MULTIPLIERS

The two multipliers that produce the in-phase and quadrature components, were constructed from high frequency double-balanced mixers, (Philips, 1988) and exhibit excellent phase characteristics and gain matching.

The phase and the amplitude, are extremely important factors, when using the phasing method for separation of sideband and in order to meet the design goal of minimum -35 dB sideband separation the phase error must be less than 2^0 (The American Radio Relay League 1992) and the voltage error must be less than 2%.

(Radio Society of Great Britain 1982).

3.2 DETAIL DESIGN CONSIDERATION

3.2.1 PLL

The design consideration for the phase lock loop where it maintains lock down to at least -10 dB signal to noise ratio (white noise). This value was chosen as it can be easily achieved with simple design techniques, and sufficiently below noise level, that even with maximum noise reduction the recovered audio will not be useable. In addition it must not suffer phase modulation in the presence of the following:

- Fading of signals and sidebands.
- Selective fading of carrier and sidebands.
- Interfering signals more than 100 Hz from the wanted carrier with levels of +10 dB above it.

The importance of reducing the phase noise in the phase lock loop, is that when the phasing method is used for selection of sideband, any change in phase will cause a change in signal amplitude, which will reduce sideband separation, and increase noise. The requirement for handling +10 dB interfering signals was done in order to utilise the +12 dB headroom (headroom - the ability of the system to handle impulse signals above its normal operation point without saturation) built into the system.

The loop must be able to follow spurious hum (induced 50 Hz and 100 Hz from the mains power supply that causes unwanted interference to the local oscillators, it can appear as AM, FM, or both), synthesizer noise (FM noise, generated by the voltage controlled oscillator "hunting" the reference oscillator), poor

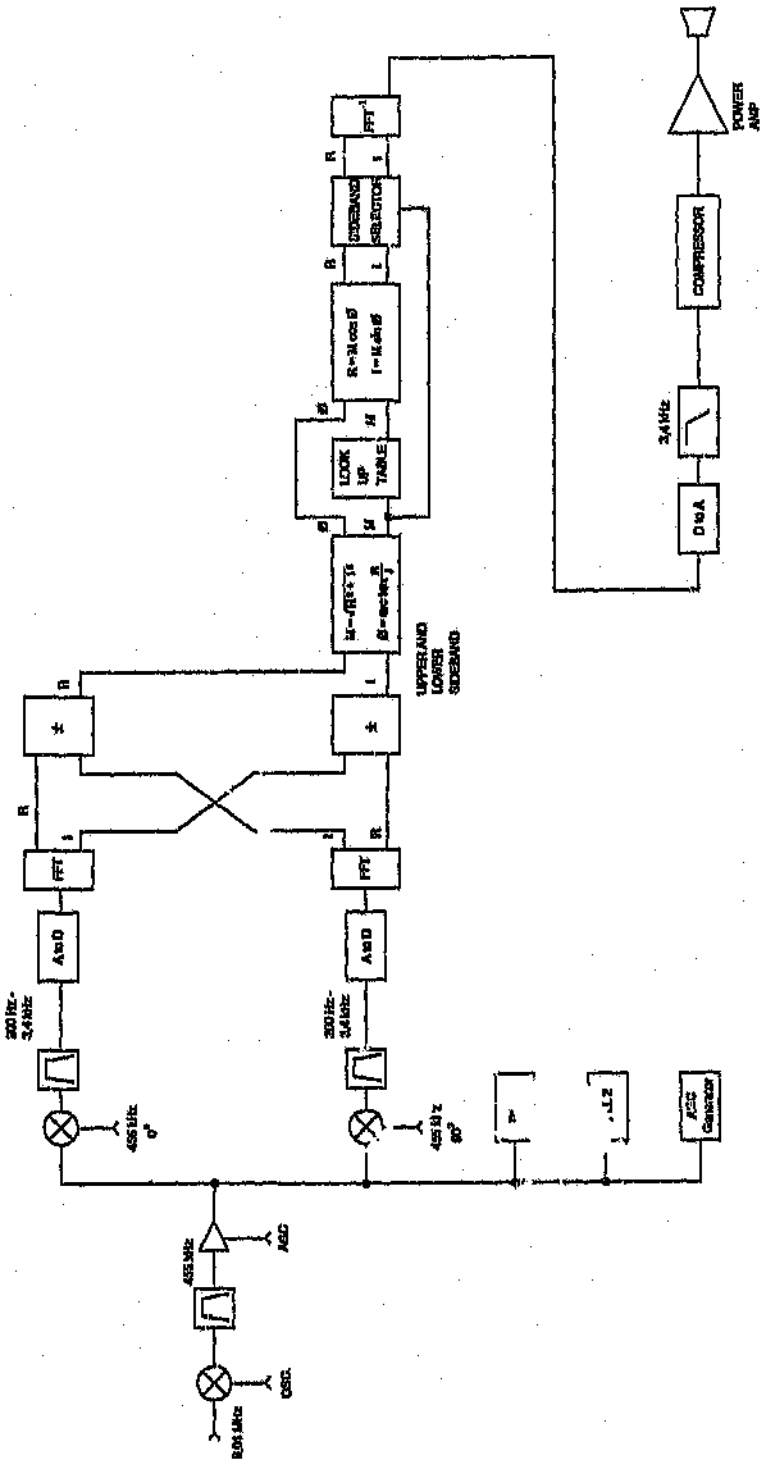


FIGURE 3.1 : BLOCK DIAGRAM

3.1.1 GENERAL DESCRIPTION OF THE NEW DETECTOR

The block diagram of the new detector is shown in Figure 3.1. The IF output of 9,01 MHz is converted to 455 kHz. The phase-locked-loop and the two multipliers, perform synchronous demodulation for in-phase and quadrature components.

The two analog signals are converted into 16 bit digital signals in the A to D converters (Sheingold, D.H. 1986) and from that point on, all processing will be done digitally.

The two signals enter to 256 points FFT (Brigham, E.O. 1976), which act as a filters bank, with time constant equal to the inverse of the bandwidth of each point. The real and the imaginary components, computed by the FFT, are added and subtracted from each other in order to generate the upper and lower sidebands (Zavrel, R.J. Jr. 1985), and then converted to phase and magnitude in the pythagoras processor. The sideband selector, selects the sideband with the lowest magnitude (point 2 of the design goal) selection, of the quietest signal ensures that interference on one side band are eliminated, as long as they are not present at the same frequency on both side bands.

A non linear look up table changes the magnitude (point 1 of the design goal), and the polar to cartesian converter (Plessey Semiconductors, 1990b), converts the signal to real and imaginary and after the inverse FFT process, the digital to analog converter (DAC) produces an analog audio signal.

APPENDIX A:
Figure 32: Same as in Figure 31 after DSP operation.

APPENDIX A:
Figure 33: Same as in Figure 31 after sideband selection.

Note 40 dB reduction in the 800 Hz interference and about 37 dB reduction in the 2,5 kHz interference.

APPENDIX A:
Figure 34: Same as in Figure 33 with the addition of noise reduction level set to 8.

Note that both interfering signals are well suppressed into the background noise level.

The next test was done in order to show the reduction of interference in addition to white noise.

APPENDIX A:
Figure 35: The incoming signal consists of:
- Carrier with no modulation, 250 kHz, 1mV peak.
- Interference 252,5 kHz, 250 µV peak.
- Interference 249,2 kHz, 250 µV peak.
- White noise 10 mV peak.

The plot was taken after the synchronous detector.

APPENDIX A:
Figure 36: The signal as in Figure 35 after sideband selection.

Note 15 dB reduction in interfering signals and about 3 dB reduction in white noise level. The noise reduction mode was not used because of the absence of modulation. Without a signal which is stronger than the noise, the compressor will simply amplify the expended noise to its original value, and no noise reduction will take place.

APPENDIX A:

Figure 27: Signal consisted of carrier at 250 kHz 1 mV peak modulated with 1 kHz, 100% modulation. Interference at 252,5 kHz, 250µV peak (which will give upper sideband interference of 2,5 kHz). The signal is recorded at the output of the synchronous detector.

The harmonic distortion seen in the plot were produced by the signal generator, and not by the circuit.

APPENDIX A:

Figure 28: Same as in Figure 27 after passing the DPS.

APPENDIX A:

Figure 29: Same as in Figure 27 after sideband selection.

Note 34 dB deduction in the 2,5 kHz interference.

Figure 30: Same as in Figure 29 with the addition of noise reduction level at 8.

Note the interfering signal wa reduced to noise level. Re-doing the last two tests after the compressor circuit was modified, resulted in about 9 dB reduction in 3rd harmonic distortion. Further testing was done with two high quality Marconi signal generators, (one for the signal and one for the interference), instead of the H.P. multifunction generator with 12 bit accuracy. The result was that the 3rd harmonic was only about 8 dB above noise level.

APPENDIX A:

Figure 31: Same signal as in Figure 27 with the additional interference at 249,2 kHz with a level of 250 µV peak (-800 Hz from the carrier) output of the synchronous detector.

APPENDIX A:

Figure 21: Same signal as in Figure 16, but with 50% modulation, noise at 10mV peak and carrier at 1mV stayed the same. Output is taken from the analogue synchronous detector.

Note that the harmonic distortion produced by the signal generator, is reduced and covered by noise.

APPENDIX A:

Figure 22: Same signal as in Figure 21, taken after DSP pass with no alteration.

APPENDIX A:

Figure 23: Same input as in Figure 21 after sideband selection.

APPENDIX A:

Figure 24: Same input as in Figure 21 after sideband selection and noise reduction at level 4.

APPENDIX A:

Figure 25: Same as in Figure 21 with noise reduction at level 6.

APPENDIX A:

Figure 26: Same as in Figure 21 with noise reduction at level 8.

Note a reduction of about 16 dB in noise level.

The next set of tests were done with continuous interference.

APPENDIX A:
Figure 15: The signal as in Figure 11 with noise reduction set to level 8.

Note improvement of about 13 dB in white noise level, comparing to synchronized detector.

APPENDIX A:
Figure 16: Signal as in Figure 6 with noise level increased to 10mV peak, measured after the synchronous detector.

The 2nd and 3rd harmonics are generated by the signal generator.

APPENDIX A:
Figure 17: The signal as in Figure 16 after DSP operation.

APPENDIX A:
Figure 18: The signal as in Figure 16 after automatic sideband selection.

APPENDIX A:
Figure 19: The same as Figure 16 with the addition of noise reduction set to level 4.

APPENDIX A:
Figure 20: The signal as in Figure 16 with noise reduction set to level 8.

Note about 14 dB improvement in signal to noise ratio over synchronous demodulation.

Higher level of noise could not be tested, as it caused saturation of the A to D converters. Reduction of signal level would also not help since the synchronous AGC will increase gain, and the ratio between signal and noise will stay the same. The solution to this problem, was to leave the carrier at the same level, and to reduce the modulation.

APPENDIX A:
Figure 7 : Signal as in Figure 6 after DSP but without noise reduction.

APPENDIX A:
Figure 8 : Same as in Figure 6 with sideband selection.

Note about 5 dB improvement in signal to noise ratio.

APPENDIX A:
Figure 9 : Same as in Figure 6 with noise reduction switch at position 4.

APPENDIX A:
Figure 10: Same as in Figure 6 with noise reduction switch at position 8.

APPENDIX A:
Figure 11: Same signal as in Figure 6 but with noise level increased to 4 mV peak, measured after the synchronized detector.

The 2nd and 3rd harmonics are generated by the signal generator, and not by the circuit and the plot, gives accurate representation of the signal at the antenna terminal.

APPENDIX A:
Figure 12: The signal as in Figure 11 after DSP operation.

APPENDIX A:
Figure 13: The signal as in Figure 11 after sideband selection.

APPENDIX A:
Figure 14: The signal as in Figure 11 with the addition of noise reduction which is set to level 4.

APPENDIX A:

Figure 1 : The 1 kHz signal after the analogue synchronized detector.

APPENDIX A:

Figure 2 : The 1 kHz signal after passing the DSP section with Blackman-Harris operator and without any noise reduction operation.
(A to D → FFT → FFT^{-1} → D to A)

APPENDIX A:

Figure 3 : The 1 kHz signal after automatic sideband selection.

Note the reduction in noise and 2nd and 3rd harmonics level.

APPENDIX A

Figure 4 : The 1 kHz signal with noise reduction switch at position 4.

APPENDIX A:

Figure 5 : The 1 kHz signal with noise reduction switch at position 8.

Investigation into the large increase in 3rd order harmonic distortion, discovers that it was generated in the compressor stage (Ref 47), and not in any of the DSP operations. After completing all the tests described in this chapter, the circuit was modified in order to correct a small DC level shift that caused the problem. After trimming the circuit the 3rd harmonic dropped by 11 dB.

APPENDIX A:

Figure 6 : Signal as in Figure 1, with the addition of 1 mV peak white noise.

Note the effect of the low pass filter cutting at 3,4 kHz.

4.2 RF SIMULATION TESTS

The following tests were conducted:

1) Clean signal, in order to check proper operation.

2) Signal with various levels of white noise in order to show noise reduction.

3) Signal with continous interference, in order to show the effectiveness of the side band selection.

4) Combination of white noise and continuous interference. This test shows the effectiveness of the complete system.

5) Frequency modulated interference, in order to determine the effect of FM station transmitting inside the passband of the AM station.

The detector was connected to an ICOM R70 receiver, which was tuned to a frequency of 250 kHz. The antenna input of the receiver was fed from an HP multifunction signal generator, and the audio output of the detector, was monitored by an HP spectrum analyzer, with 10 Hz resolution.

The signal generator was set to generate an A.M. signal with carrier of 250 kHz at 1mV peak, with 100% modulation of 1 kHz.

The following results were recorded:

In order to solve the above problems, a change was made in order to allow full overlapping of the FFT, i.e. complete FFT after every incoming sample. The result was that audio distortion was completely eliminated and some improvement in white noise level could be heard. The improvement in continuous interference was unchanged.

The last section to be tested in the initial testing was the expandor-compressor. It did create some changes in audio characteristics, for the following reasons:

1) The Blackman-Harris window operator has a large number of side-lobes. As a result of the expansion process, during single tone testing, the main frequency bin was left unaffected but the secondary side-lobes, which has much lower amplitude were attenuated.

2) During multitone tests, the largest signal stays at the same magnitude, due to the compressor circuit, but weaker signals are attenuated. This of course is a desirable effect, which proves the proper operation of the circuit, but nevertheless creates an audible change.

4. RESULTS

This chapter will give the results of the tests conducted on the new detector. It starts with initial tests of the sub-section of the circuit, and then describes the system tests with ICOM R70 receiver.

4.1 PRELIMINARY

The circuit was designed and constructed in order to prove the theory. The first tests were conducted with the circuit functioning as a synchronized detector only, with the digital circuits bypassed. White noise test shows that PLL1 operated properly down to about +10 dB signal to noise ratio. It maintained lock down to about +2 dB but with increased phase noise. PLL2 operated down to -10 dB, which is the design limit, with excellent phase noise. The AGC maintained constant output to within 1dB with input changes of over 60 dB. After proving the successful operation of the analogue section, the digital section was activated.

Initial testing was done with FFT, with no overlapping, and Blackman-Harris operation. Speech passing through the system suffered from distortion and white noise testing indicated approximately 3 dB degradation in noise level. On the other hand, continuous interference was successfully eliminated. Investigation into the increase in noise level found that the white noise tends to be averaged out during the FFT operation, and the 32 ms window was sufficiently long that the noise in both upper and lower sidebands had approximately the same level. As a result the sideband switching circuitry did not function and the circuit operated as one sideband detector which led to 3 dB degradation in signal to noise ratio.

In addition the wrong signal will always be in a level less than the signal. When the interference is in opposite phase and in magnitude higher than twice the signal, the correct sideband is selected.

Figure 3.2 demonstrates the problem. The signal level is fixed at +10 and the interference level can vary.

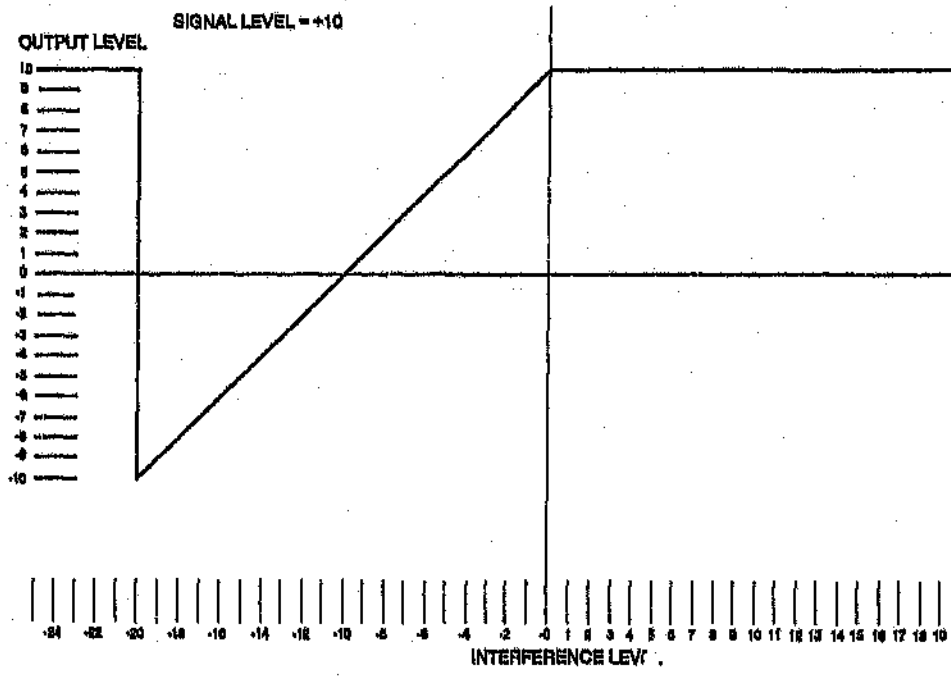


FIGURE 3.2 : OUTPUT VERSUS INTERFERENCE

will be presented at the input to the FFT, and the quality of the wanted signal be degraded to some extent.

In practice, the operation of the detector, will be limited by the ability of the phase lock loop to lock on the wanted carrier. The design goal was handling ~ 10 dB of white noise and, -10 dB continuous interference, 100 Hz or more, away from the wanted carrier. Improving the PLL any further, will not have any benefit, since the output signal to noise ratio from the detector, will be too low to be usable.

3.3.4 PROBLEM DUE TO SIDEBAND SELECTION

The sideband selection system will give rise to another problem. If at a particular bin of the FFT, the interference is in the same phase as the signal, the sideband with the interference will be stronger and the other sideband will be selected. On the other hand if the interference is in the opposite phase, it will reduce the amplitude and the wrong sideband will be selected. When the interference is equal in magnitude to the signal, but opposite in phase, the output will be zero. It is obvious that when the choice is to have high level interference or "hole" in the spectrum, the hole will be much less noticeable.

The real problem happens, when the interference is equal to twice the level of the signal, and opposite in phase. The output will start increasing, but in opposite phase. It is difficult to predict to what extent this out of phase signal will interfere with audio quality, but is a known phenomena. that the human hearing is not sensitive to phase distortion (Craiglow, R.I., 1963).

The FFT algorithm has 16 bit input with block floating point and conditional scaling. With this configuration, the maximum tone with respect to noise, is 74 dB, slot noise test is 61 dB and 2 tone with frequency spread is 63 dB. (Plessey Semiconductors 1990). Other DSP operations, contribute very little to loss in dynamic range, comparing to the FFT, and can be ignored.

(Slot noise test : a measurement in which white noise is passed through a narrow band notch filter, several frequency bins wide, and the FFT computed. There is no noise in the filtered slot at the input to the FFT, but there is noise in the frequency bins corresponding to the width of the notch. Dynamic range is measured as the difference in dB of the average signal power and the average noise power).

(2 tone with frequency spread : a measurement in which two sinusoids of different amplitudes, with the larger one residing mid-way between two frequency bins, and the smaller 5.5 bins away. The dB figure is the difference in amplitude between the two signals when the smaller one is still just detectable as a separate peak from the larger one).

It is clear from the above results that the maximum theoretical dynamic range is slightly over 60 dB or 10 bits (ignoring PLL operation). Setting the wanted signal to a level of -10 dB, reduces this figure to some extent. Due to changes in signal strength and AGC operation, this level can vary and should be regarded as average only. If no interference is present, the 14 bit input will only have a marginal effect on the performance of the FFT, since the block floating point will compensate for the unused bits, but if strong interference is present, full 16 bits

H.P. 8903B Audio Analyzer was used in order to measure SINAD (signal, noise and distrotion). This type of measurement was preferred over signal to noise ratio, since it also measured the distortion generated by the last two operations.
The results of the tests are tabulated in the following table:

SINAD (dB)	ICOM R70 (μV) Signal Level	SYNCHRONOUS DEMODULATION (μV) Signal Level	SIDEBAND SELECTION (μV) Signal Level	SIDEBAND SELECTION AND NOISE REDUCTION AT POSITION 6 (μV) Signal Level
31				1,0
29,5				0,9
28				0,8
27				0,7
25,5				0,6
24				0,5
22,5				0,4
19				0,3
15	1,05	0,96	0,92	
14	0,85	0,8	0,77	
13	0,74	0,7	0,68	0,2
12	0,64	0,62	0,59	
11	0,55	0,54	0,51	
10	0,49	0,48	0,44	0,17
9	0,43	0,44	0,39	
8	0,38	0,38	0,35	0,15
7	0,33	0,32	0,30	
6	0,30	0,29	0,29	
5	0,27	0,24	0,25	
4	0,24	0,20	0,20	
3	0,2	0,18	0,17	
2	0,15			

and magnitude (Figure 25).

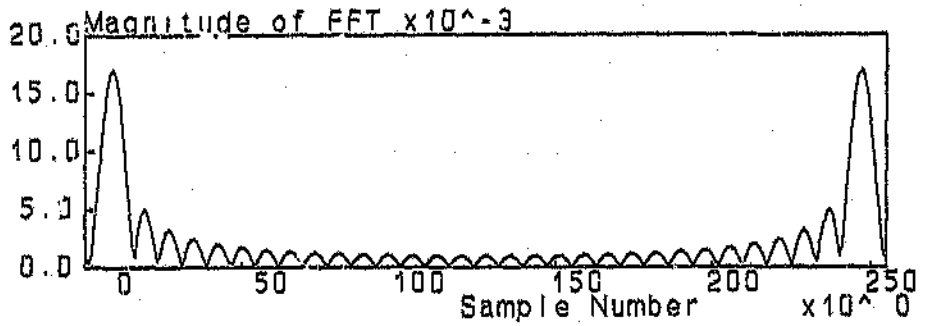


FIGURE 25

Note that the two FFT's are different from each other, and as a result good sideband separation cannot take place.

The above example was simplified in order to demonstrate the problem. In a real system the ratio between the carrier and the audio frequencies will be much higher, and the interfering pulse will have an attack and decay time after passing the IF filter.

4.4 RECEIVER SENSITIVITY TEST

The receiver was connected to a Marconi RF signal generator, generating signal at 2,1 MHz modulated with 1 kHz at 80% modulation. The audio was monitored at four points:

- detected by the ICOM R70.
- detected by the synchronous demodulator
- after sideband selection
- after sideband selection and noise reduction at position 8.

and after filtering (Figure 22).

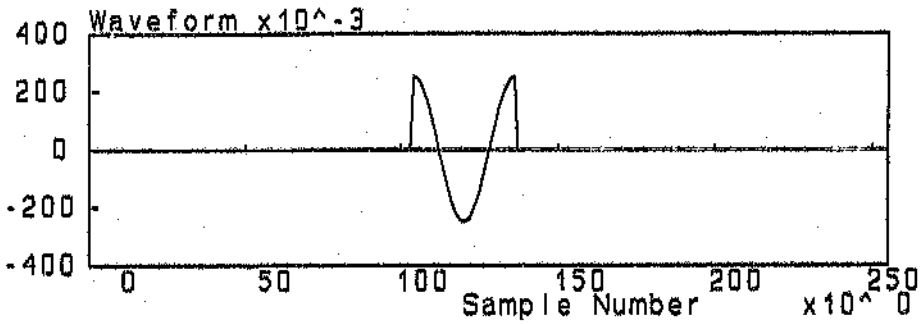


FIGURE 22

Its FFT gives real (Figure 23),

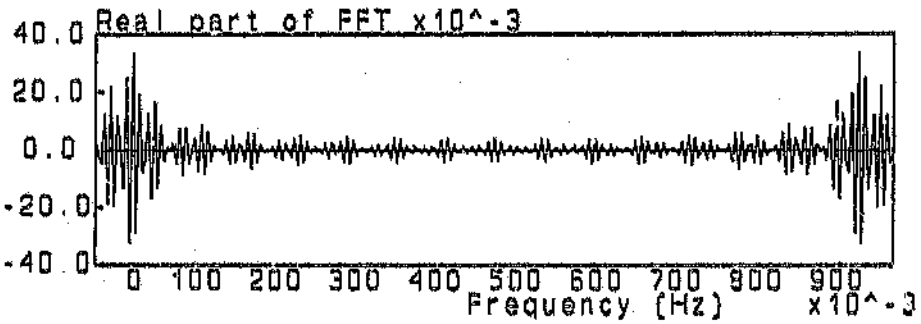


FIGURE 23

imaginary (Figure 24),

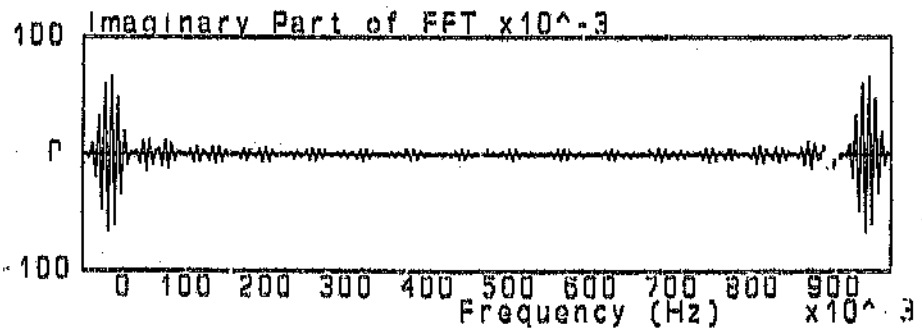


FIGURE 24

real (Figure 19),

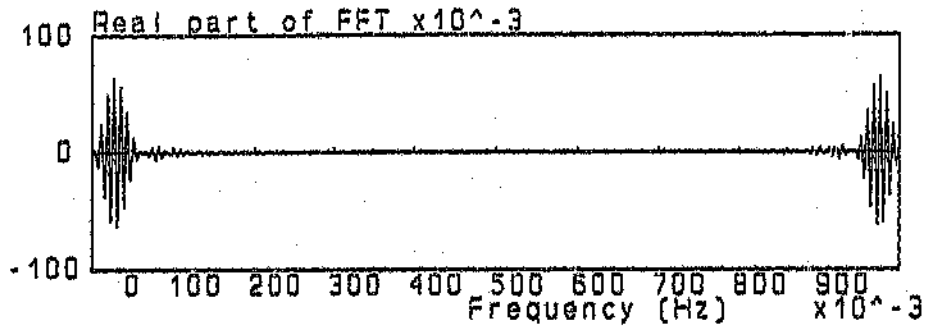


FIGURE 19

and imaginary (Figure 20).

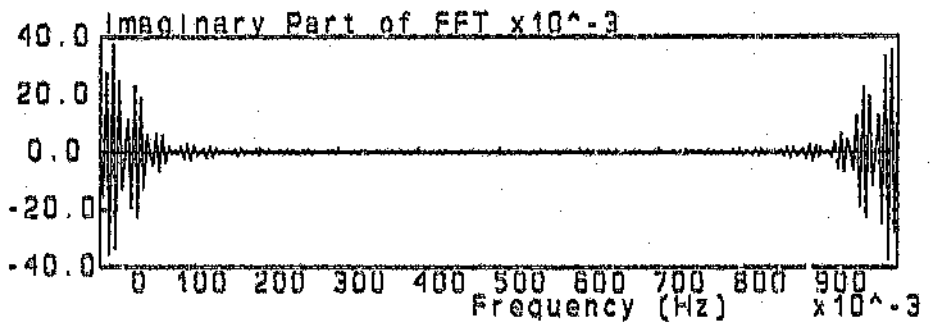


FIGURE 20

The same RF signal after multiplying by 90° (Figure 21.)

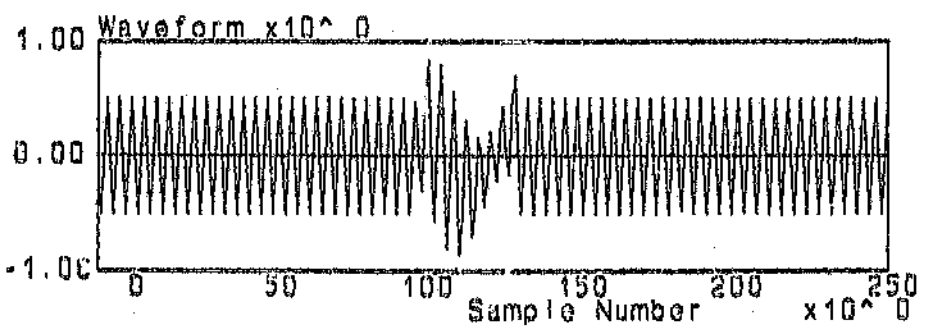


FIGURE 21

multiplied by 0° (Figure 16),

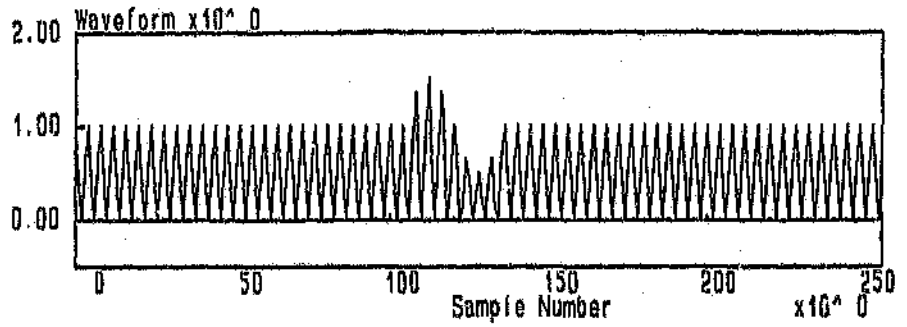


FIGURE 16

after filtering (Figure 17),

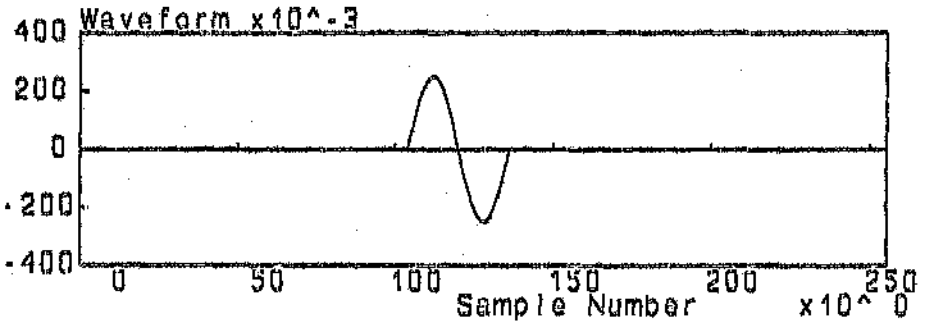


FIGURE 17

and its FFT magnitude (Figure 18),

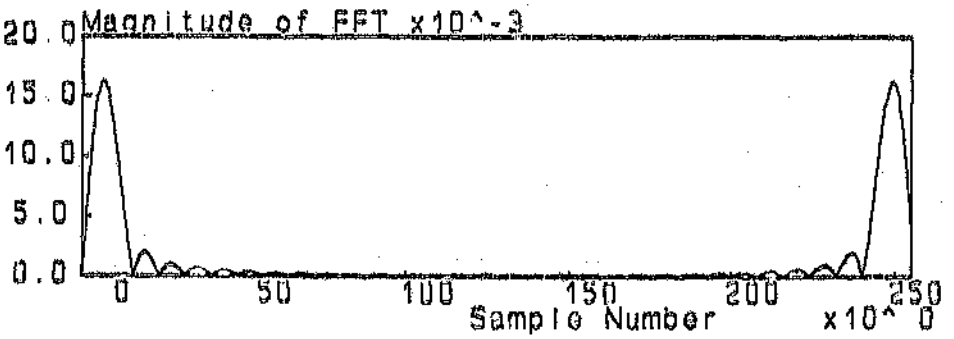


FIGURE 18

Note that the FFT's of the two signals are exactly 90° from each other and having the same magnitude. The result is that the phasing method will give perfect sideband cancellation, and the interference will be eliminated.

If the signal is random or does not occupy the full length of the FFT window, the situation is different.

Let's assume a short burst of the above interfering signal Figure 14,

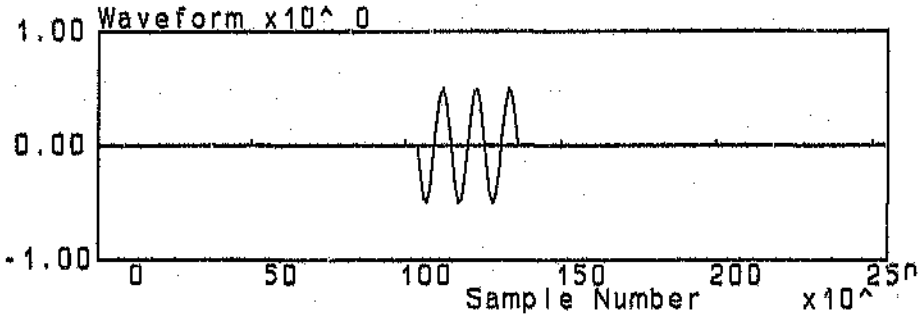


FIGURE 14

added t e carrier, Figure 15,

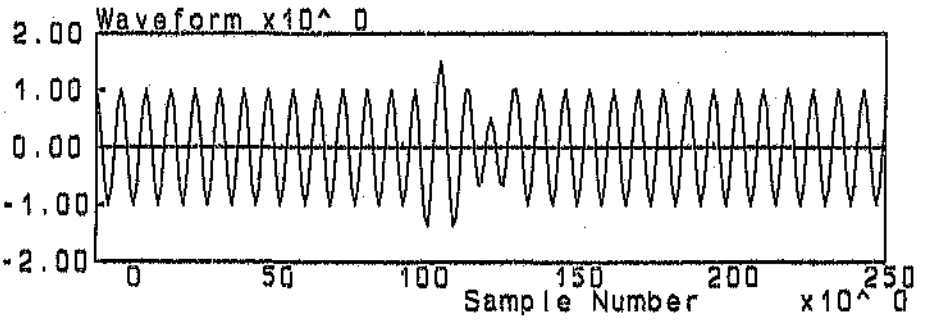


FIGURE 15

Its FFT real is Figure 11,

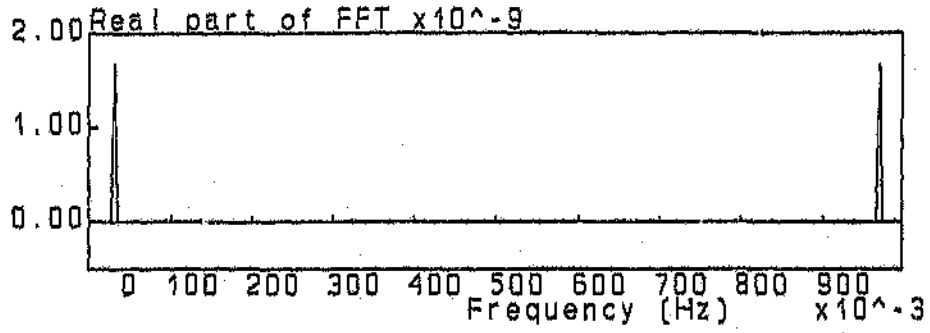


FIGURE 11

imaginary Figure 12

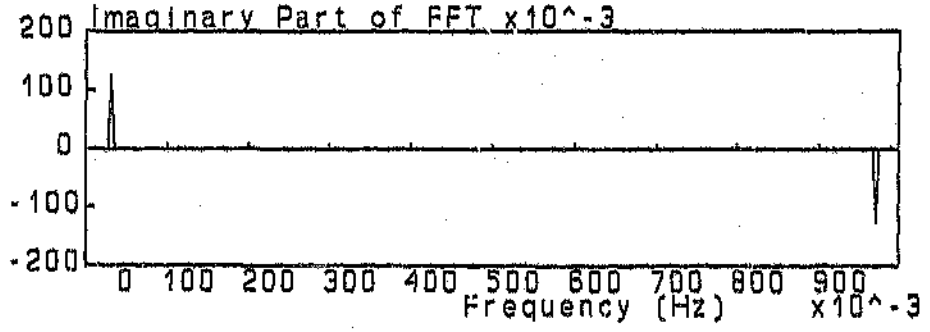


FIGURE 12

and magnitude Figure 13,

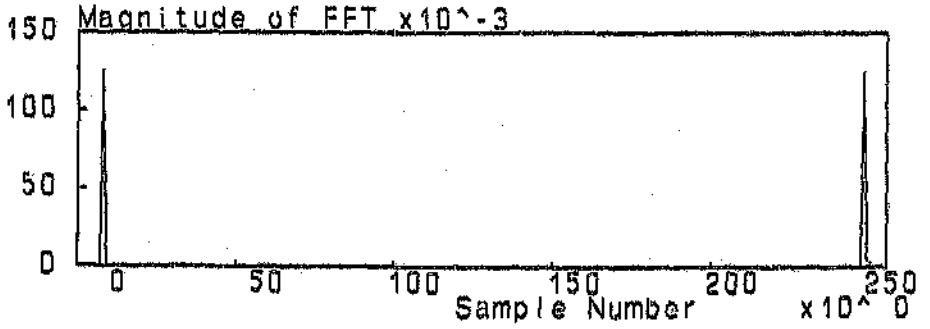


FIGURE 13

and imaginary components Figure 8.

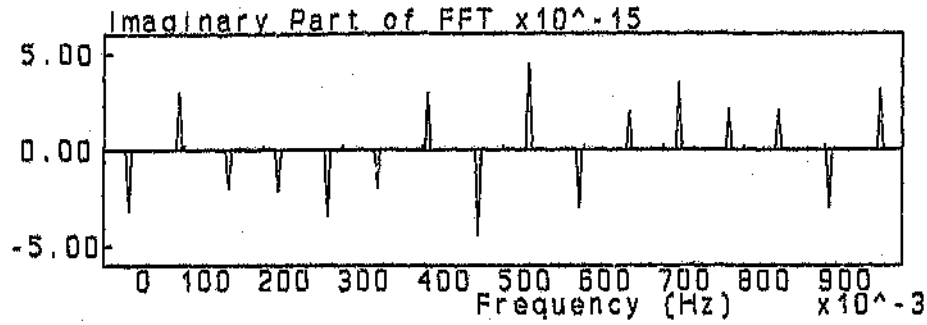


FIGURE 8

After multiplying the RF signal with the carrier with 90°, we get Figure 9

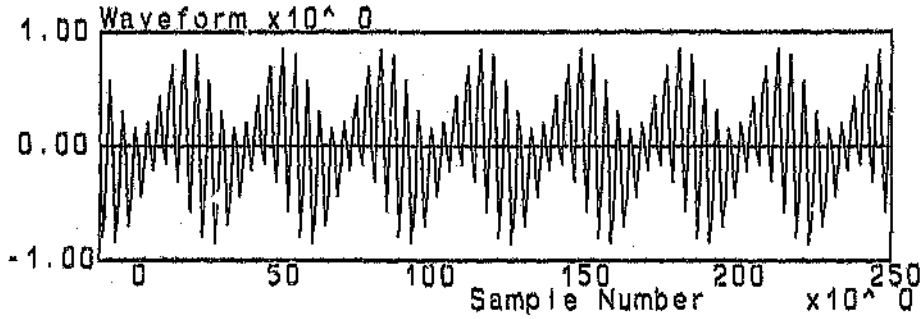


FIGURE 9

and after filtering Figure 10.

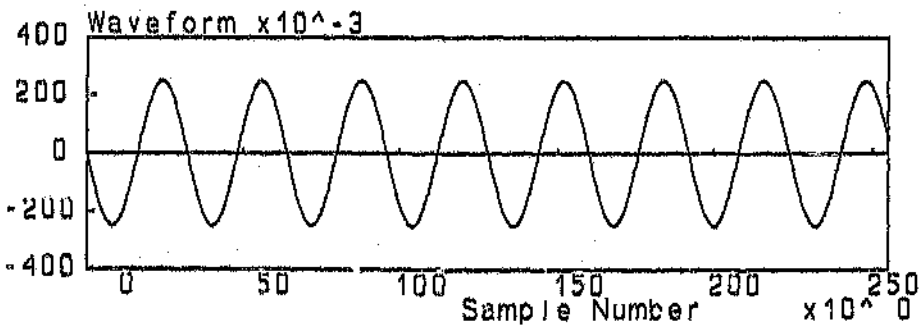


FIGURE 10

and after filtering and removing the DC, Figure 5

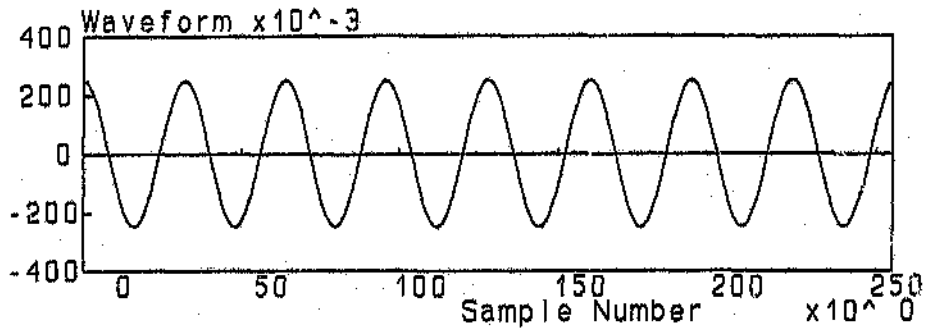


FIGURE 5

and its magnitude FFT, Figure 6

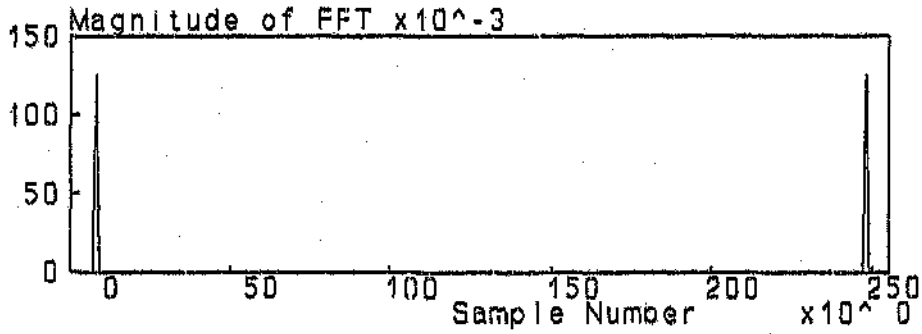


FIGURE 6

real components, Figure 7

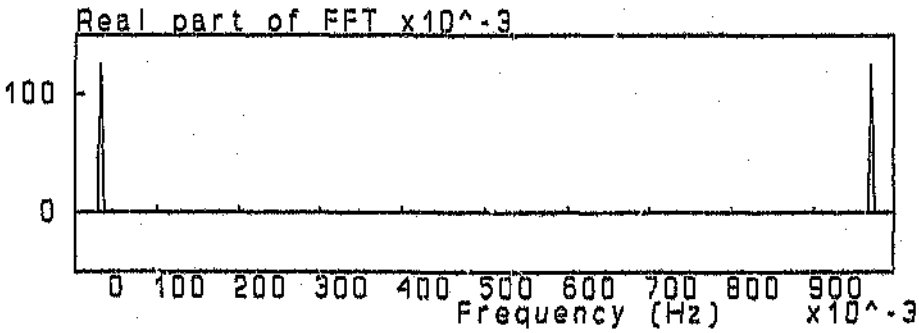


FIGURE 7

and continuous interference (Figure 2).

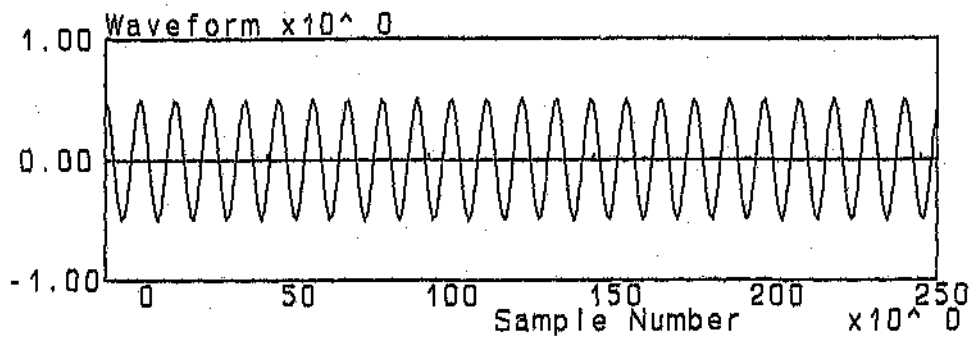


FIGURE 2

The combined signal is as shown in Figure 3.

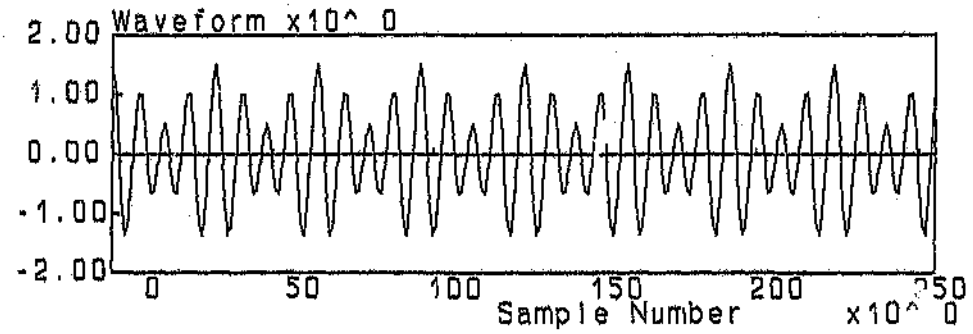


FIGURE 3

After multiplying with the carrier with 0^0 we get Figure 4

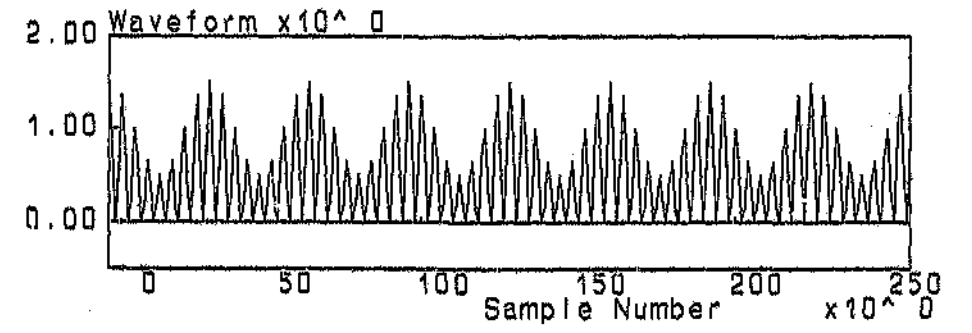


FIGURE 4

4.3 ANALYSIS

The tests shows that the new detector is very efficient in reducing continuous interference. Wideband noise at one sideband was also substantially reduced. The effect of the sideband selection on white noise, distributed equally on both sidebands, was not large, and the noise reduction mode was used with good results.

The large reduction of continuous interference (>35 dB) compared to the small reduction in discontinuous interference, white noise, (≈ 5 dB) led to further investigation. It was found that the phasing method, used for sideband separation, was not a good choice.

Lets assume a signal with a carrier (Figure 1);

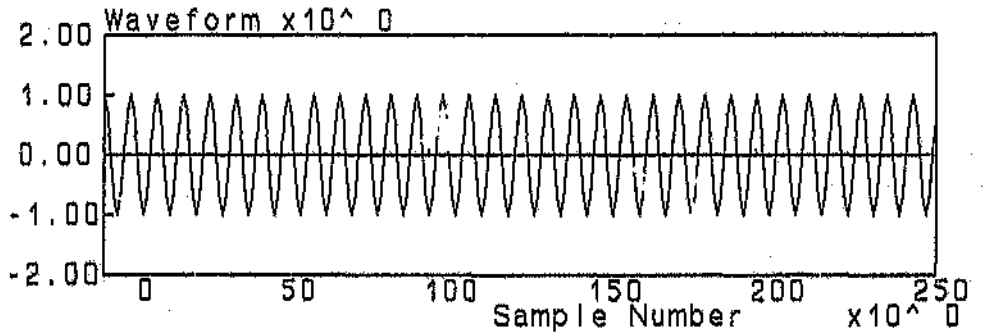


FIGURE 1

The next test was aimed to measure the effect of an FM interfering signal, effecting one sideband only.

APPENDIX A:
Figure 37: Signal consisted of:

- Carrier of 250 kHz, 1 mV peak, no modulation.
- Interference of FM modulated signal of 252 kHz, 1 mV peak, modulated by white noise, ± 2 kHz deviation. The plot was taken after the synchronous detector.

APPENDIX A:
Figure 38: The signal as in Figure 37 after sideband selection.

Note reduction of 39 dB in the 2 kHz interference from the carrier and large reduction in noise from FM sidebands.

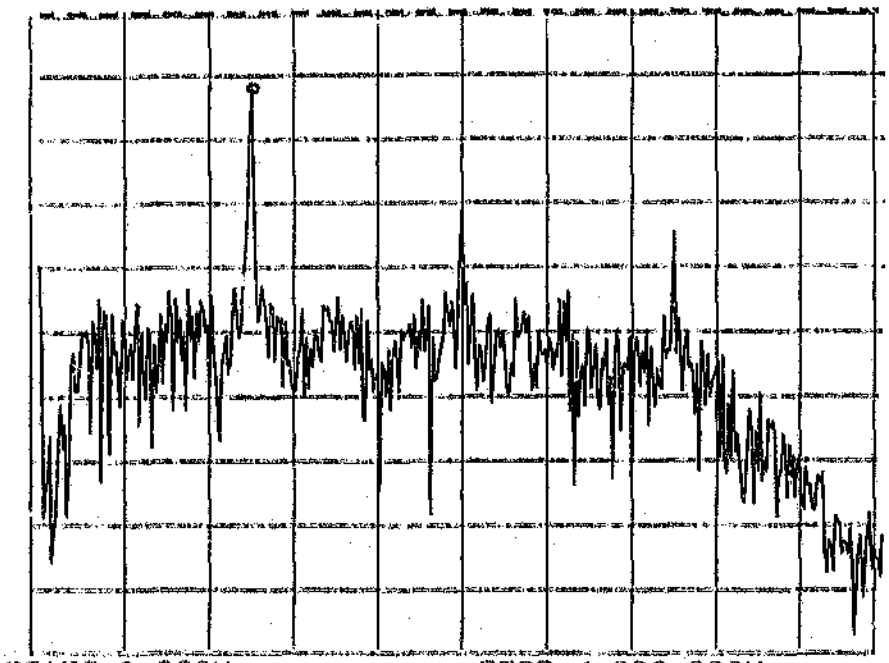
APPENDIX A:
Figure 39: The signal of Figure 37 with deviation of ± 25 kHz in order to effect both sidebands. The plot was taken at the antenna terminal with 8 kHz span.

APPENDIX A:
Figure 40: The signal as in Figure 39 after synchronous detector.

APPENDIX A:
Figure 41: The signal as in Figure 39 after sideband selection.

Note about 25 dB improvement around 2 kHz sloping down to about 10 dB at the edges of the passband.

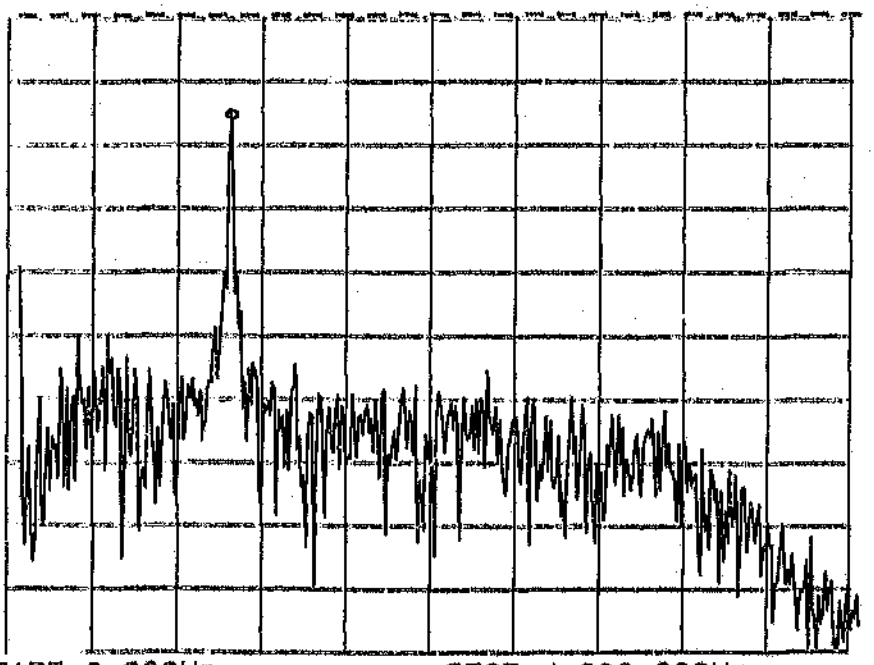
REF LEVEL /DIV MARKER 1 010.000Hz
-5.000dBm 10.000dB MAG (A) -16.723dBm



START 0.000Hz STOP 4 000.000Hz
AMPTD -10.0dBm

FIGURE 13

REF LEVEL /DIV MARKER 1 010.000Hz
-5.000dBm 10.000dB MAG (A) -20.623dBm



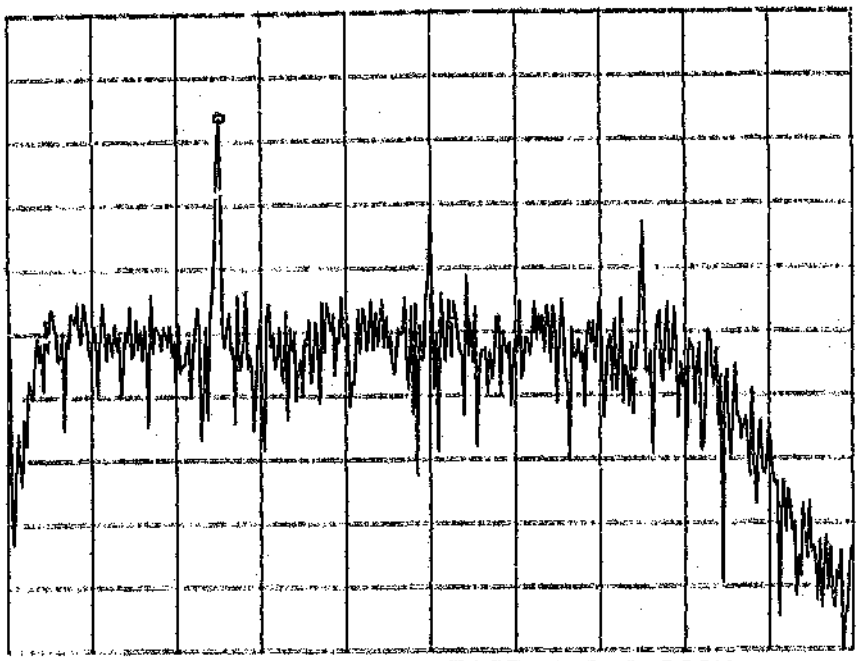
START 0.000Hz STOP 4 000.000Hz
AMPTD -10.0dBm

FIGURE 14

REF LEVEL
-6.000dBm

/DIV
10.000dB

MARKER 1 010.000Hz
MAG (A) -21.184dBm



START 0.000Hz
AMPTD -10.0dBm

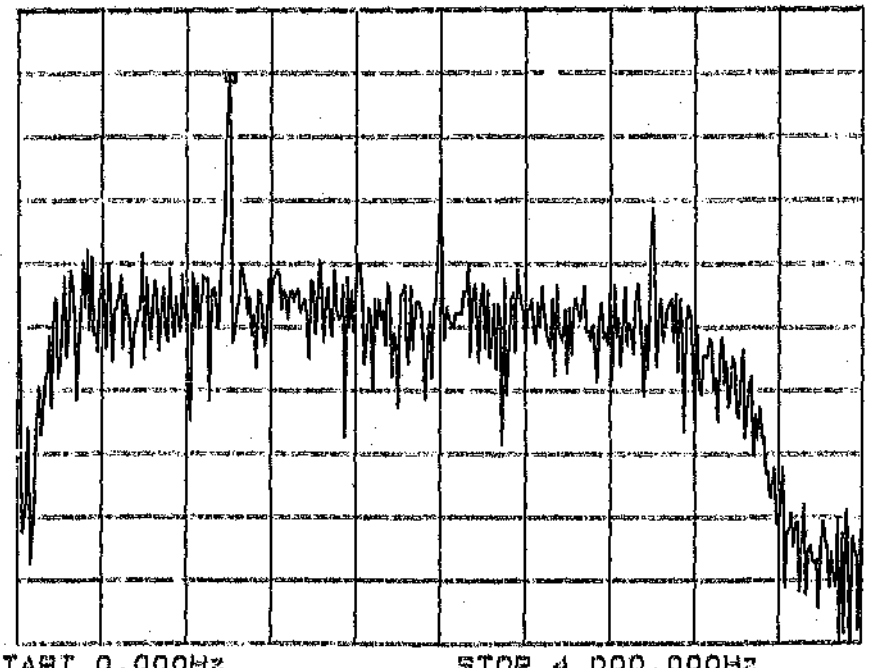
STOP 4 000.000Hz

FIGURE 11

REF LEVEL
-6.000dBm

/DIV
10.000dB

MARKER 1 010.000Hz
MAG (A) -15.698dBm

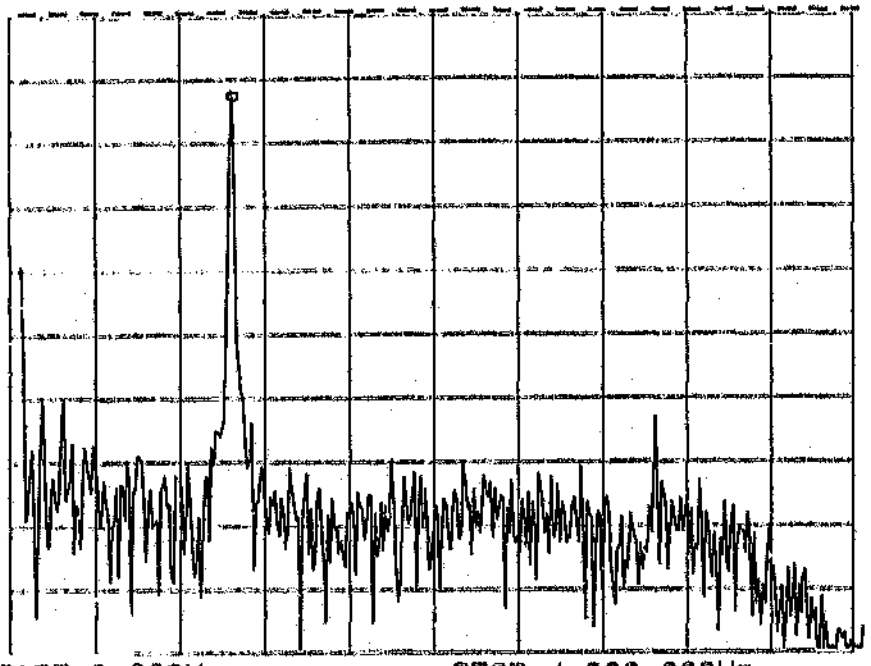


START 0.000Hz
AMPTD -10.0dBm

STOP 4 000.000Hz

FIGURE 12

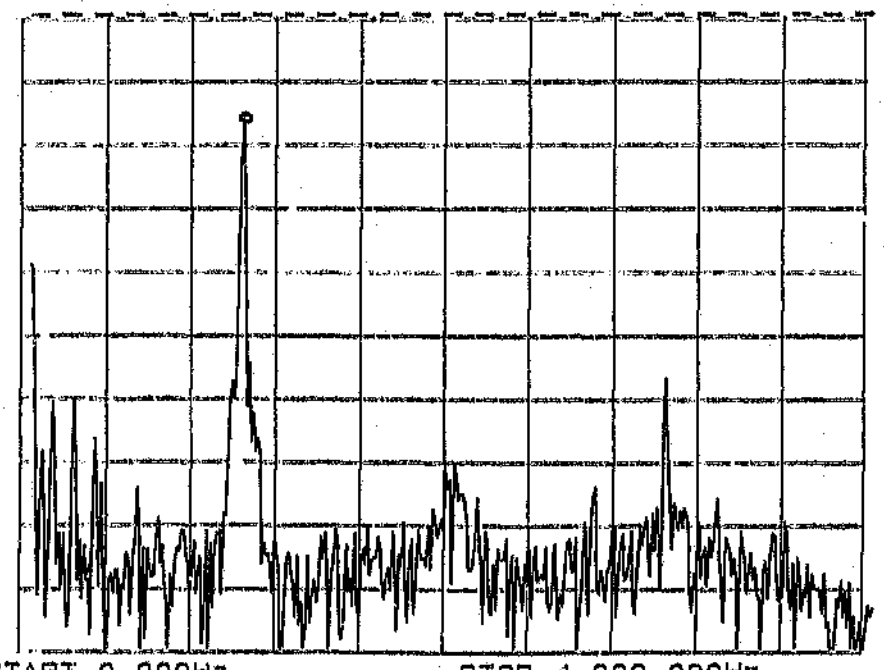
REF LEVEL /DIV MARKER 1 010.000Hz
-5.000dBm 10.000dB MAG (R) -16.054dBm



START 0.000Hz STOP 4 000.000Hz
AMPTD -10.0dBm

FIGURE 9

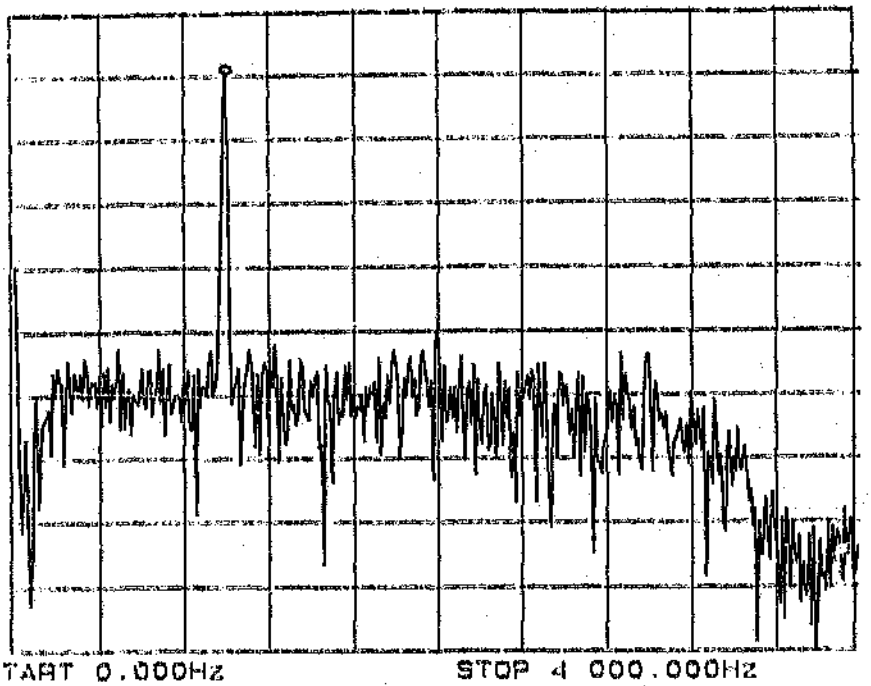
REF LEVEL /DIV MARKER 1 010.000Hz
-5.000dBm 10.000dB MAG (R) -21.192dBm



START 0.000Hz STOP 4 000.000Hz
AMPTD -10.0dBm

FIGURE 10

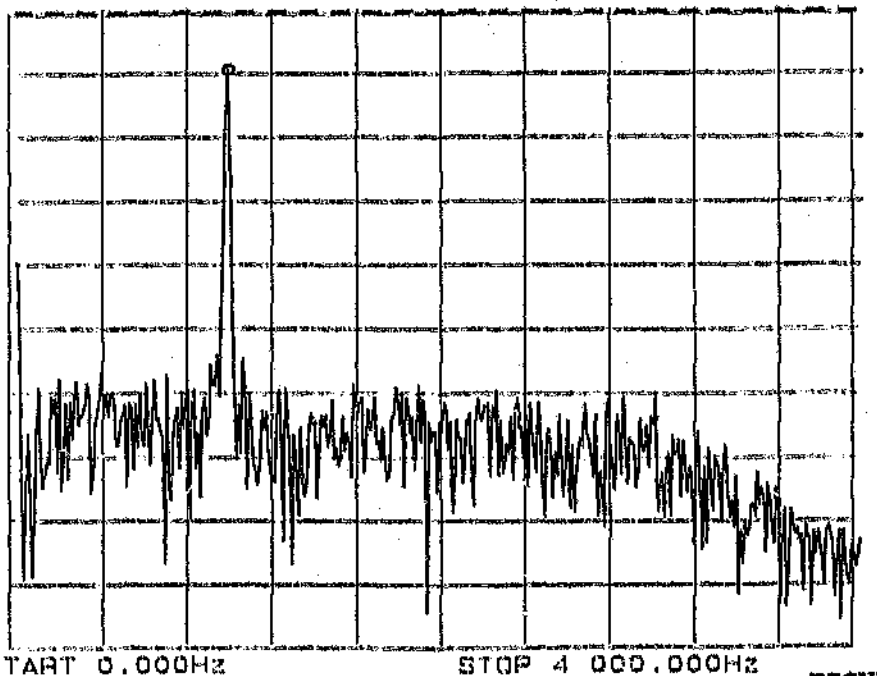
REF LEVEL /DIV MARKER 1 010.000Hz
-5.000dBm 10.000dB MAG (R) -13.731dBm



START 0.000Hz STOP 4 000.000Hz
AMPTD -10.0dBm

FIGURE 7

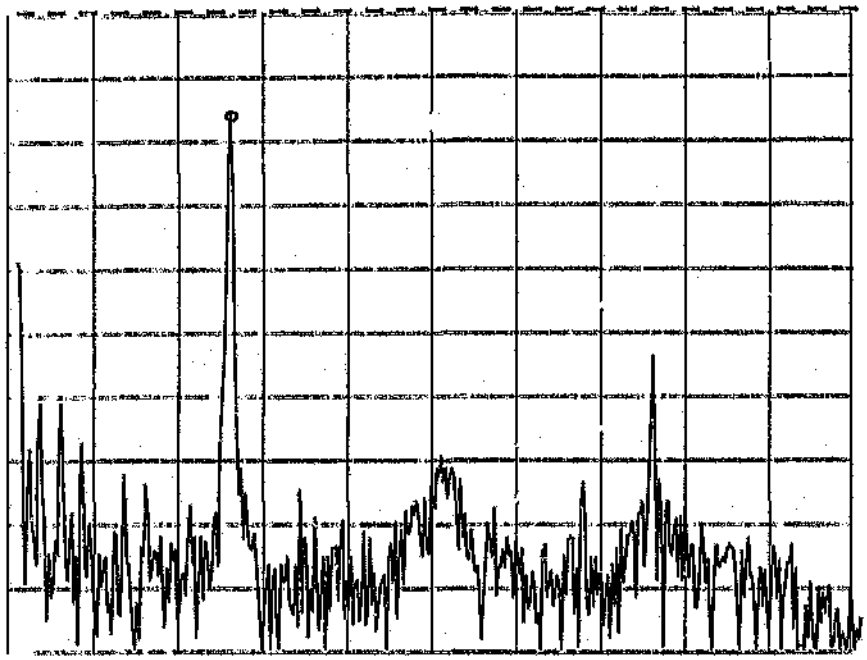
REF LEVEL /DIV MARKER 1 010.000Hz
-5.000dBm 10.000dB MAG (R) -14.026dBm



START 0.000Hz STOP 4 000.000Hz
AMPTD -10.0dBm

FIGURE 8

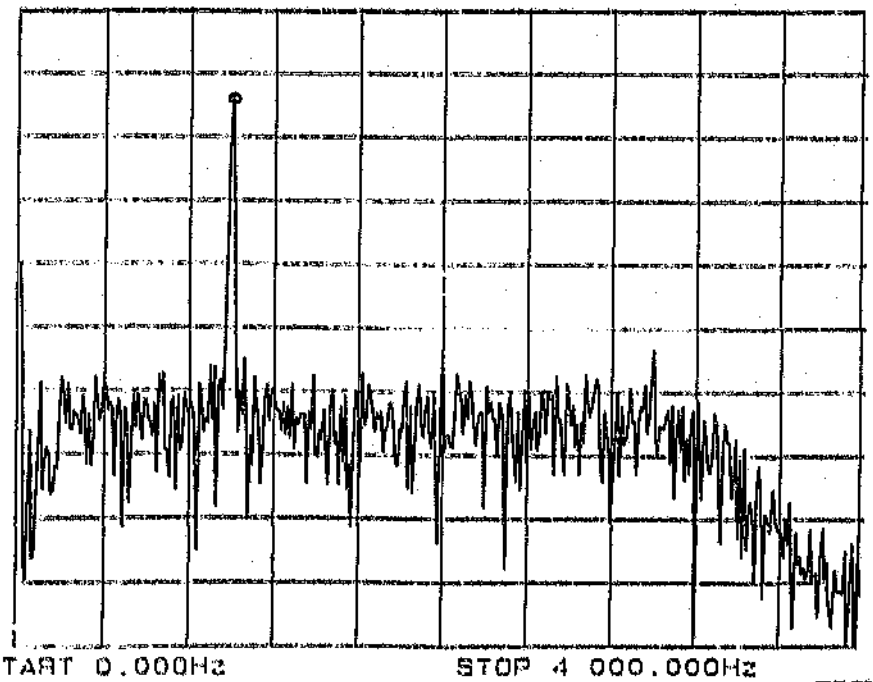
REF LEVEL /DIV MARKER 1 010.000Hz
-5.000dBm 10.000dB MAG (R) -21.371dBm



START 0.000Hz STOP 4 000.000Hz
AMPTD -10.0dBm

FIGURE 5

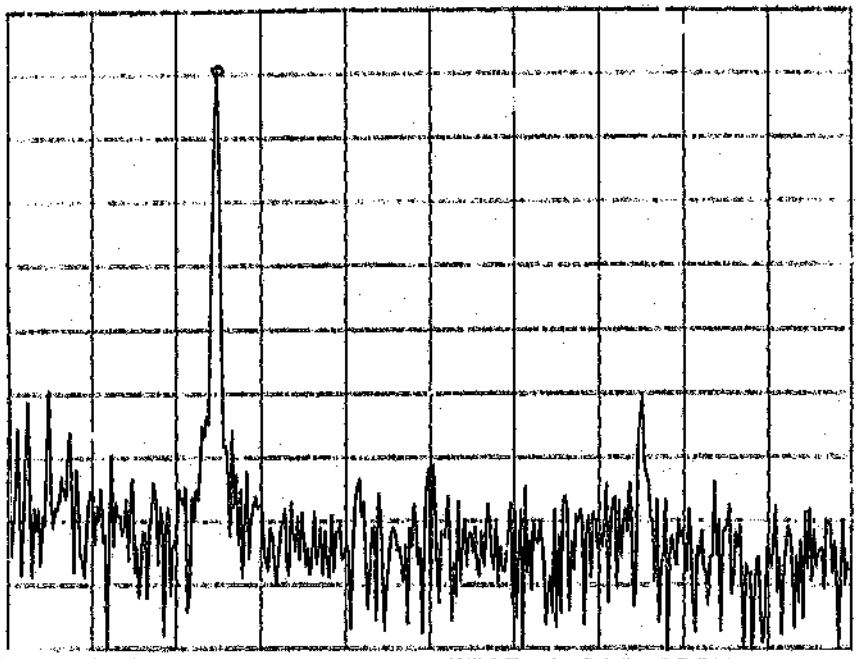
REF LEVEL /DIV MARKER 1 010.000Hz
-5.000dBm 10.000dB MAG (R) -16.765dBm



START 0.000Hz STOP 4 000.000Hz
AMPTD -10.0dBm

FIGURE 6

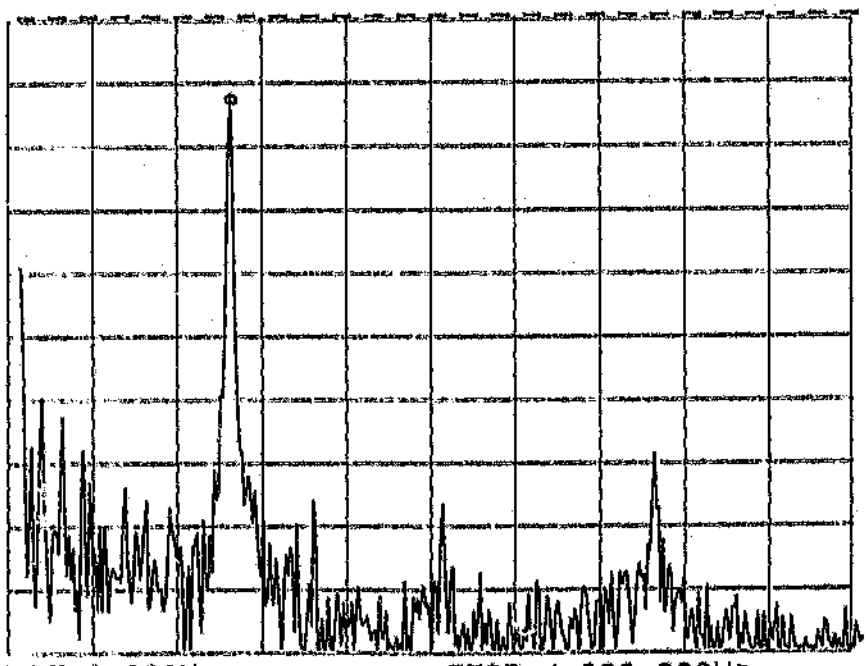
REF LEVEL /DIV MARKER 1 010.000Hz
-5.000dBm 10.000dB MAG (A) -14.110dBm



START 0.000Hz STOP 4 000.000Hz
AMPTD -10.0dBm

FIGURE 3

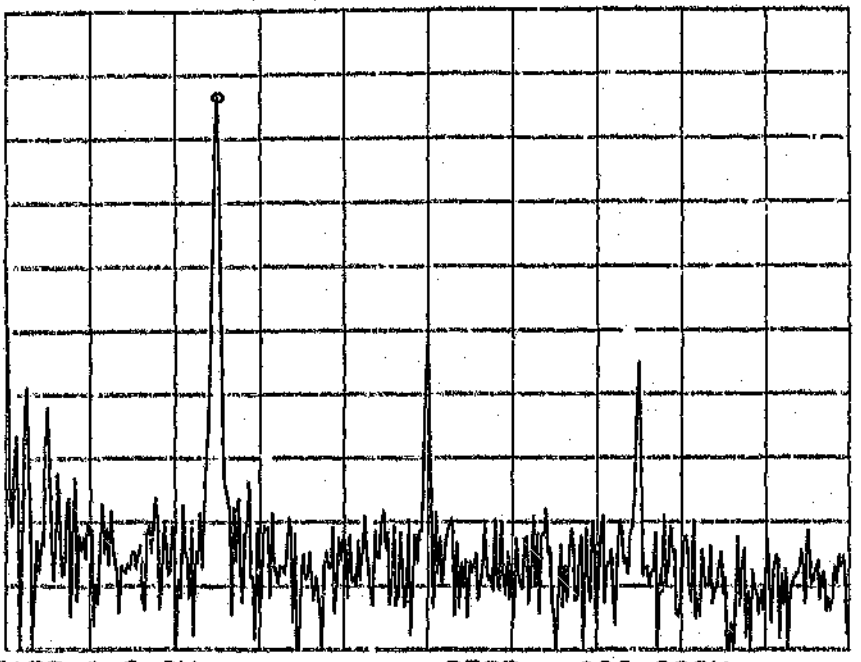
REF LEVEL /DIV MARKER 1 010.000Hz
-5.000dBm 10.000dB MAG (A) -18.045dBm



START 0.000Hz STOP 4 000.000Hz
AMPTD -10.0dBm

FIGURE 4

REF LEVEL /DIV MARKER 1 010.000Hz
-5.000dBm 10.000dB MAG (R) -18.277dBm

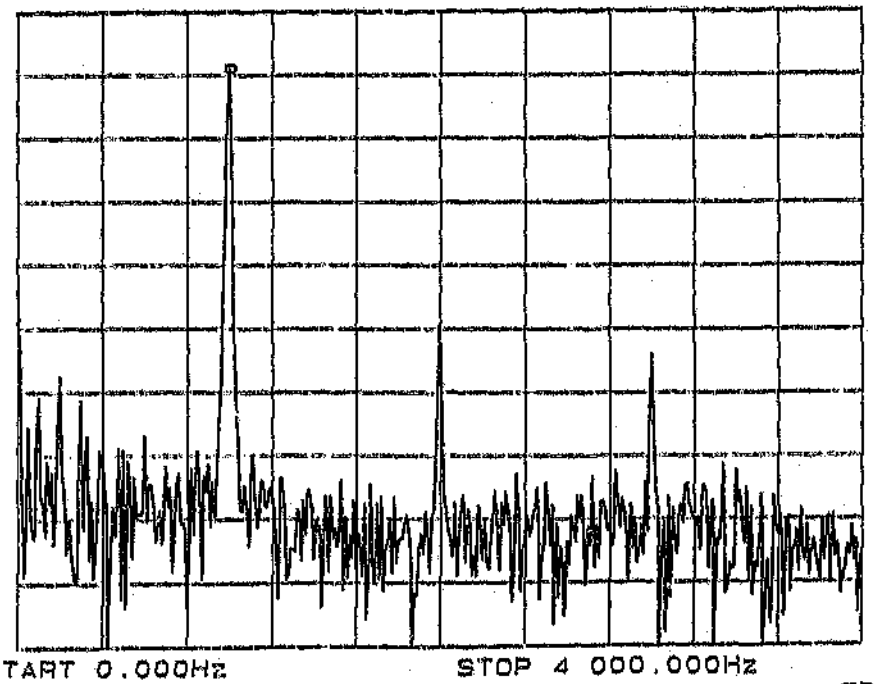


START 0.000Hz STOP 4 000.000Hz
AMPTD -10.0dBm

FIGURE 1

APPENDIX A : TEST RESULT PLOTS

REF LEVEL /DIV MARKER 1 010.000Hz
-5.000dBm 10.000dB MAG (R) -13.857dBm



START 0.000Hz STOP 4 000.000Hz
AMPTD -10.0dBm

FIGURE 2

5.3 CONCLUSION

The new AM detector offers performance far superior to the conventional detector. Its high cost will obviously limit its use to high-end receivers but as prices of DSP components are falling rapidly, the detector can find wide use in moderate price range receivers.

5.4 RECOMMENDATIONS FOR IMPROVEMENT

The concept of sideband selection proved to be a good one and can be used with other modulation techniques with two identical sidebands (e.g. FM, PM).

The circuit itself, can be improved by using DSP all the way from the IF instead of the analog circuit, but this will push up the price since the IF will have to be sampled at a very high speed.

Testing done on the ICOM R70 receiver indicates poor amplitude and phase linearities. Better performance can be expected from the present detector if a better receiver is available.

Many other important factors, for example finding the optimum FFT window, frame size and over-lapping, were not investigated due to lack of time, and further research should concentrate on those points.

The improvement is summarized in the following two tables:

NOISE LEVEL	1 mV	4 mV	10 mV	20 mV (eff.)
DIRECT	0	0	0	0
SIDEBAND SELECTION	≈ -5 dB	≈ -5 dB	≈ -5 dB	≈ -5 dB
LEVEL 4 REDUCTION	≈ -10 dB	≈ -10 dB	≈ -8 dB	≈ -9 dB
LEVEL 8 REDUCTION	≈ -10 dB	≈ -13 dB	≈ -14 dB	≈ -16 dB

TABLE 1 : OPERATION UNDER WHITE NOISE (S/N IMPROVEMENT)

Type of Interference	Direct	Sideband Selection	Level 4	Level 8
Carrier at 1 mV Mod 1 kHz at 100% 2,5 kHz from carrier interference 250 µV	-6 dB	-34 dB	-	≈ -70 dB
As above, interference 2,5 kHz and 800 Hz at 250 µV	-6 dB	≈ -38,5 dB	-	> -70 dB
FM signal with ± 2 kHz at 1 mV carrier at 1 mV.	-	≈ -40 dB	-	-
FM signal with ± 25 kHz at 1 mV carrier at 1 mV	-	≈ -35 dB	-	-

TABLE 2 : OPERATION WITH OTHER INTERFERING SIGNALS

5. CONCLUSIONS

5.1 SUMMARY OF WORK

This work demonstrated the ability to detect amplitude modulated signals with better performance than with conventional systems. The existing demodulation systems were discussed and analysed in detail in order to explain their limitations. The new detector was then presented followed by an explanation of the differences to the old methods.

The implementation of the new method was described in the design section, and the testing done on the circuit concluded the work.

A large part of the circuit was done in analogue, in order to allow easy debugging and construction at the expense of measurement accuracy, and high sensitivity to internal noise level. Many other designs and construction short cuts had to be taken due to the time restriction imposed on this project.

5.2 SUMMARY OF RESULTS

The new detector performed better than the existing detectors. In sideband selection mode it gave >35 dB reduction in continuous interference and about 5 dB reduction in white noise. The audio expender provides an additional noise reduction but at the expense of a change in audio characteristics.

higher the setting, the higher the noise. Experience shows, that the setting of this mode should be adjusted for the individual condition, in order to obtain the best audible result. It should be noted, that regardless of the setting, the improvement obtained in signal to noise ratio, is larger than the new noise and distortion, created by the circuit.

Phase lock loop 1 was useful with signals up to moderate interference and allowed easy tuning of the receiver. Strong interference caused it to generate high phase noise, which caused a reduction in side band separation. In addition it sometimes lost lock, or even worse, locked on the interfering signals. Phase lock loop 2 on the other hand, was a bit difficult to use as it required tuning the receiver to within 10 Hz of the wanted carrier. Its performance was exceptional. It always locked, and stayed locked, during all the tests, and when operating with white noise with negative signal to noise ratio, it was found that its phase noise was superior to the phase noise generated by the synthesizer of the ICOM receiver.

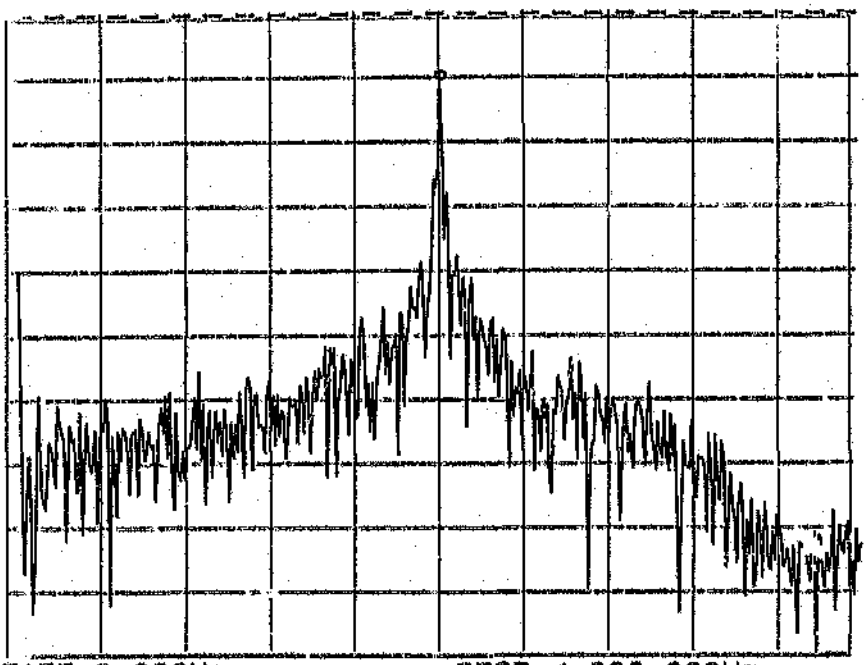
4.5 LISTENING TEST

The receiver was connected to long wire antennae, and tuned to stations in the medium and short wave bands. Strong stations sounded the same as the output from the receiver, but weak and fading stations sounded completely different. The AGC circuitry which locks on the carrier level, rather than the wide band level detection, found in ordinary receivers, was found to give a very pleasant effect when tuning to fading stations which vary in amplitude by more than 20 dB. The output level was constant, and only the changes in signal to noise ratio indicated that fading was occurring.

Stations with co-channel interference, gave spectacular improvement, particularly where the carrier of the interfering station was in the pass band. In one instance a very strong CW station was interfering about 700 Hz away from the carrier and reception from the ICOM receiver was completely unintelligible. After activating the side band selection mode, the CW station could not be heard, and the wanted station sounded as clear as a local station. This case also proves the correct operation of the AGC circuit by adjusting the level according to the wanted carrier level and not the interfering CW level.

As it was expected from the measurement, very weak signals had only small improvements from side band selection, and the noise reduction circuit had to be used. The amount of reduction in noise was directly related to the switch setting, the higher the setting the greater the improvement. The operation of this circuit had considerable effect of creating background noise that sounded like frequency modulation, the

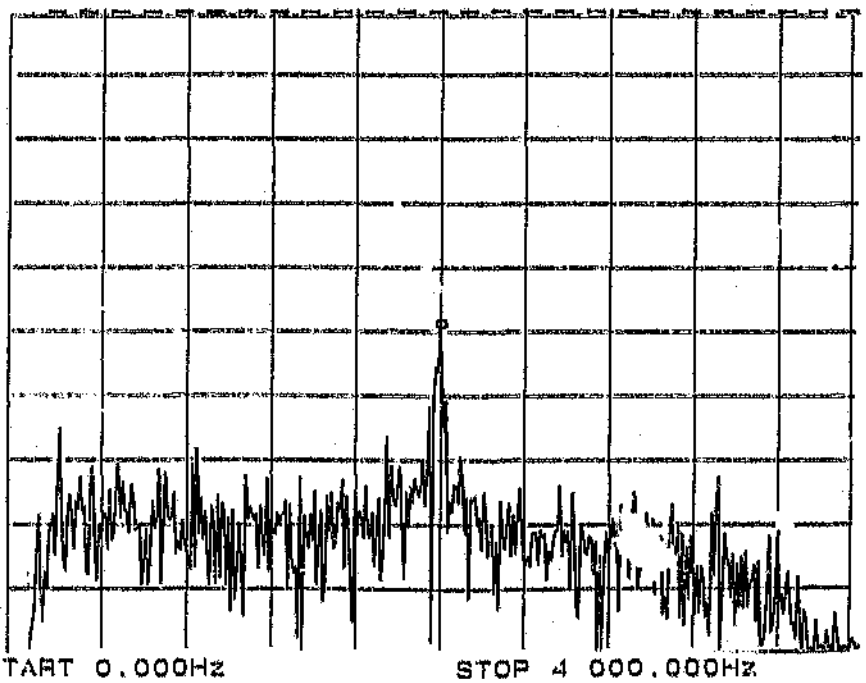
REF LEVEL /DIV MARKER 2 010.000Hz
-5.000dBm 10.000dB MAG (A) -14.521dBm



START 0.000Hz STOP 4 000.000Hz
AMPTD -10.0dBm

FIGURE 37

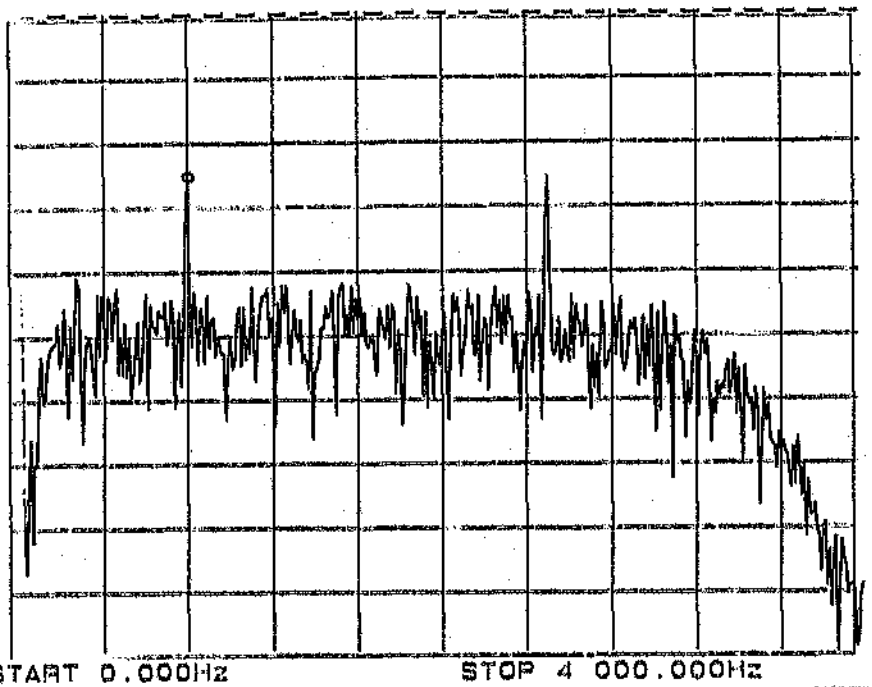
REF LEVEL /DIV MARKER 2 010.000Hz
-5.000dBm 10.000dB MAG (A) -53.878dBm



START 0.000Hz STOP 4 000.000Hz
AMPTD -10.0dBm

FIGURE 38

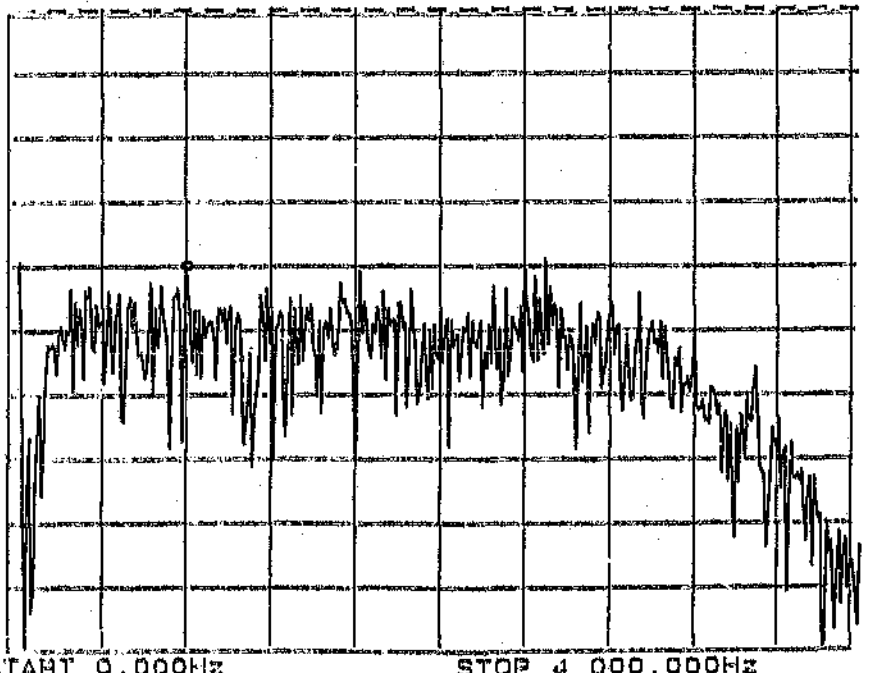
REF LEVEL
-5.000dBm
/DIV
10.000dB
MARKER 810.000Hz
MAG (A)
-30.217dBm



START 0.000Hz
AMPTD -10.0dBm
STOP 4 000.000Hz

FIGURE 35

REF LEVEL
-5.000dBm
/DIV
10.000dB
MARKER 810.000Hz
MAG (A)
-45.152dBm



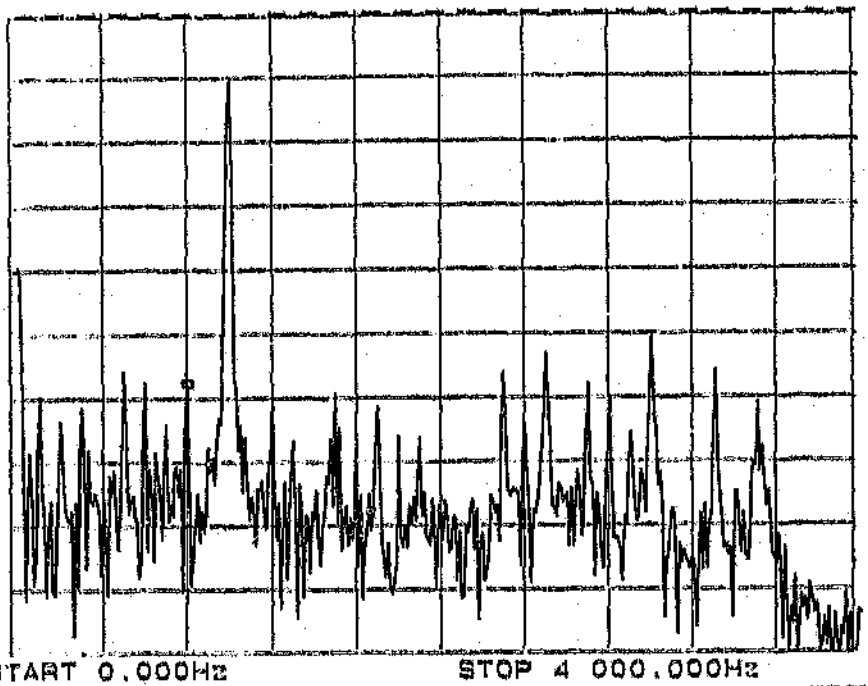
START 0.000Hz
AMPTD -10.0dBm
STOP 4 000.000Hz

FIGURE 36

REF LEVEL
-5.000dBm

/DIV
10.000dB

MARKER 810.000Hz
MAG (A) -62.828dBm



START 0.000Hz
AMPTD -10.0dBm

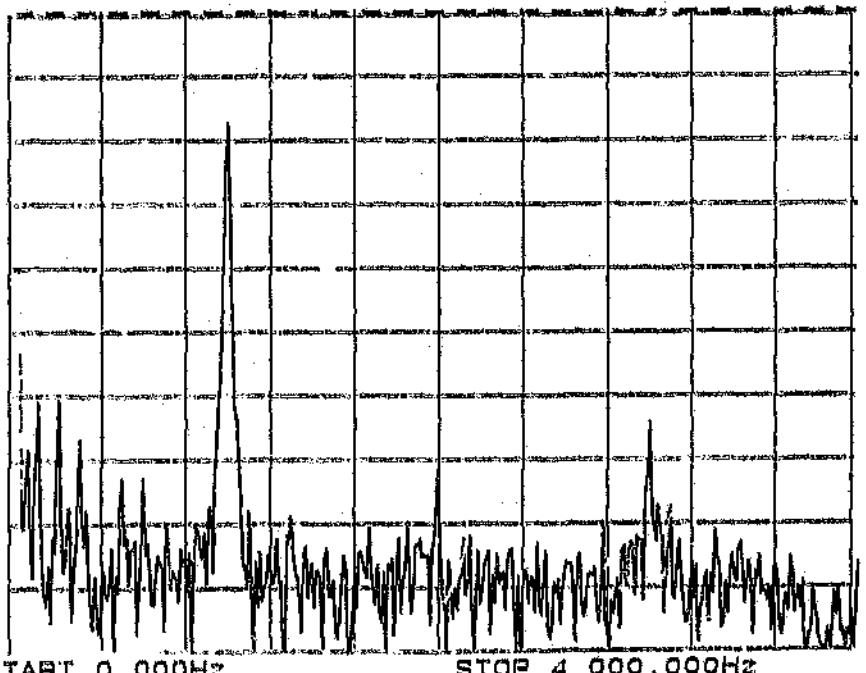
STOP 4 000.000Hz

FIGURE 33

REF LEVEL
-5.000dBm

/DIV
10.000dB

MARKER 810.000Hz
MAG (A) -91.930dBm

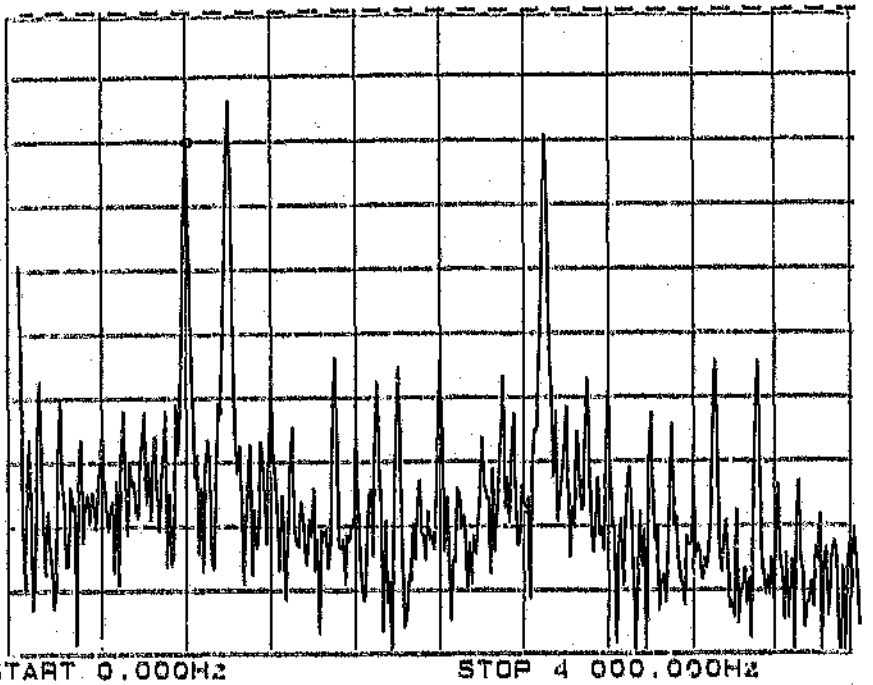


START 0.000Hz
AMPTD -10.0dBm

STOP 4 000.000Hz

FIGURE 34

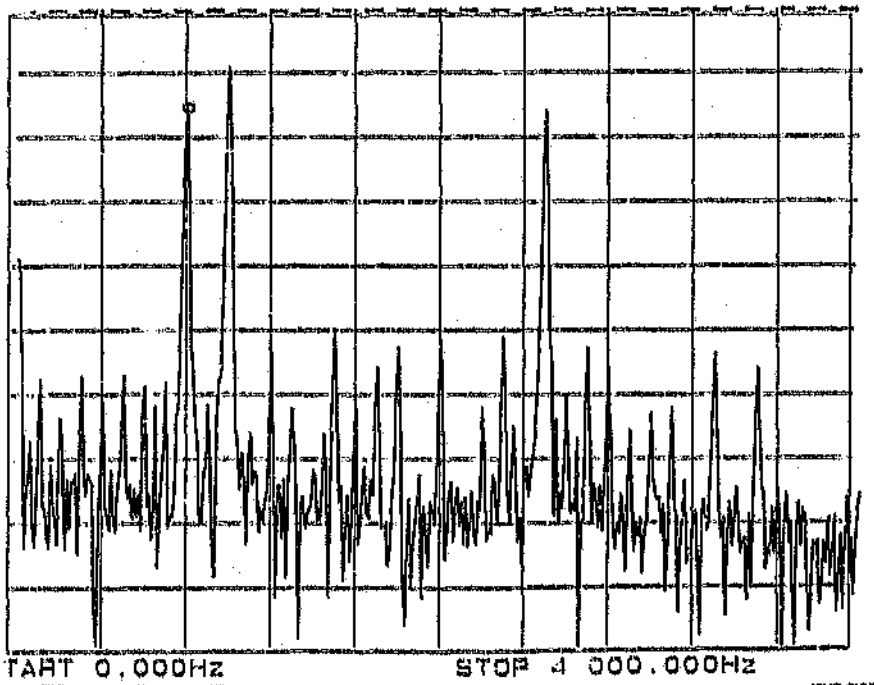
REF LEVEL -5.000dBm /DIV 10.000dB MARKER 810.000Hz MAG (R) -25.196dBm



START 0.000Hz STOP 4 000.000Hz
AMPTD -10.0dBm

FIGURE 31

REF LEVEL -5.000dBm /DI 10.000dB MARKER 810.000Hz MAG (R) -20.187dBm



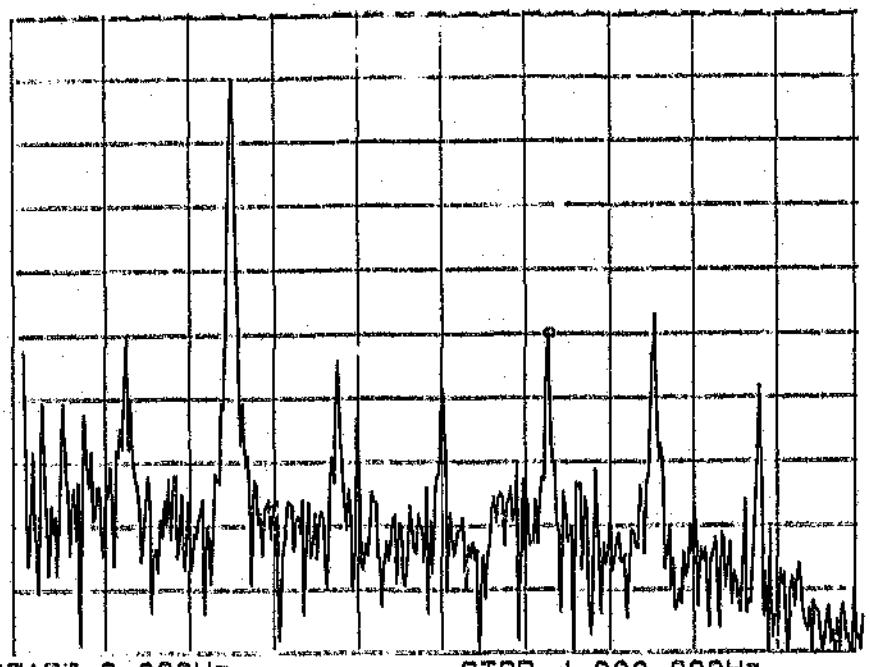
START 0.000Hz STOP 4 000.000Hz
AMPTD -10.0dBm

FIGURE 32

REF LEVEL
-5.000dBm

/DIV
10.000dB

MARKER 2 510.000Hz
MAG (R) -54.955dBm



START 0.000Hz
AMPTD -10.0dBm

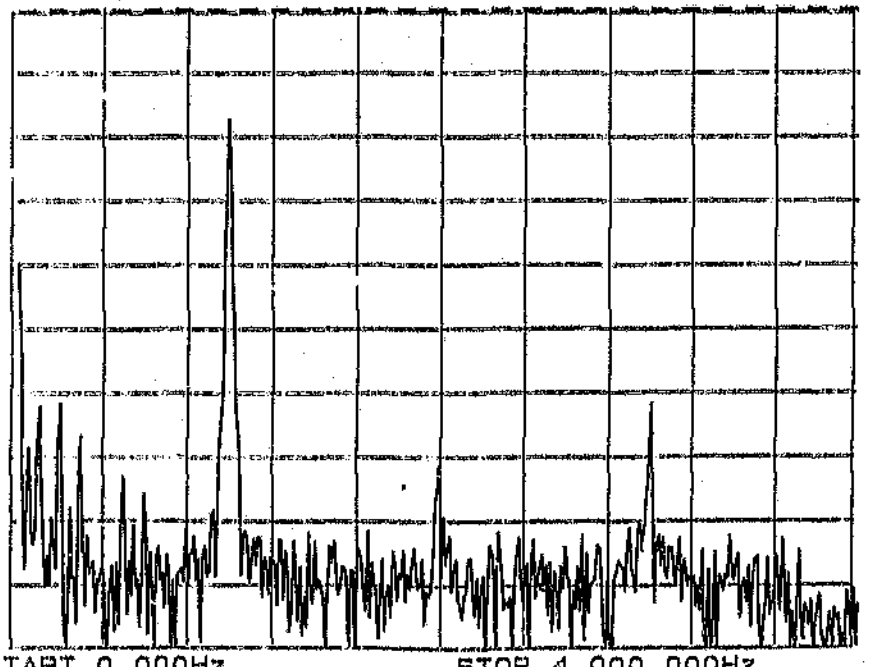
STOP 4 000.000Hz

FIGURE 29

REF LEVEL
-5.000dBm

/DIV
10.000dB

MARKER 2 510.000Hz
MAG (R) -95.355dBm

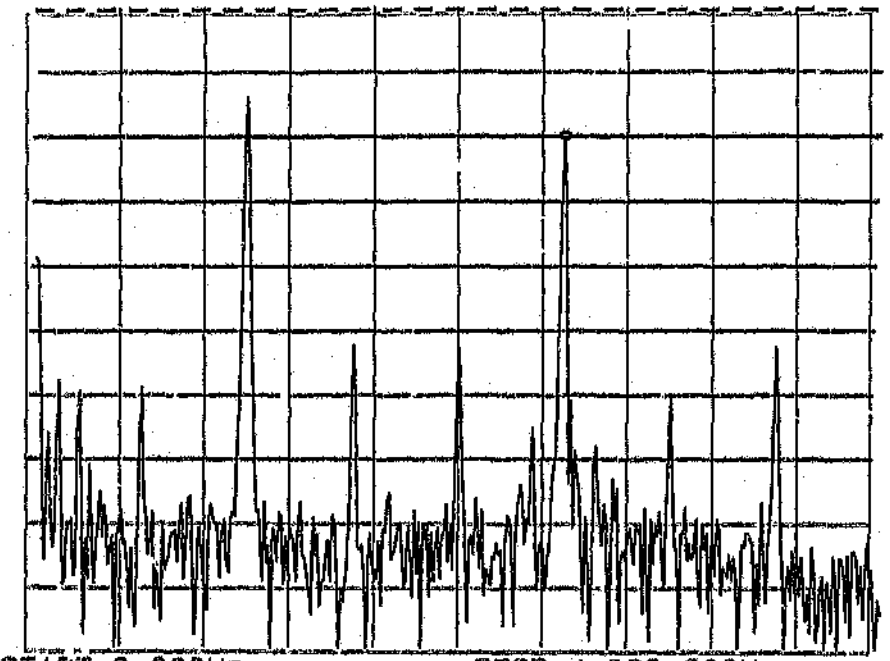


START 0.000Hz
AMPTD -10.0dBm

STOP 4 000.000Hz

FIGURE 30

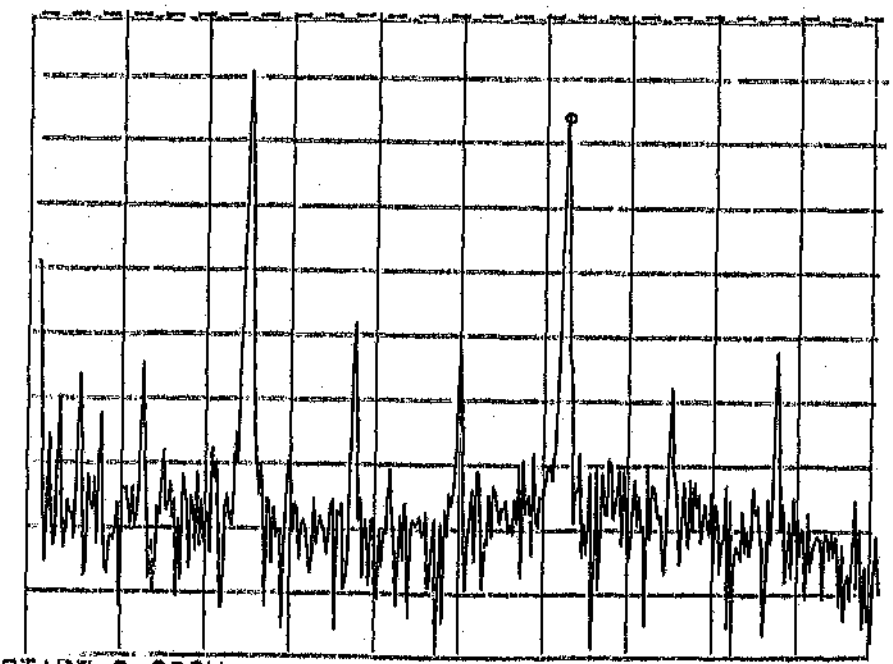
REF LEVEL /DIV MARKER 2 510.000Hz
-5.000dBm 10.000dB MAG (A) -24.628dBm



START 0.000Hz STOP 4 000.000Hz
AMPTD -10.0dBm

FIGURE 27

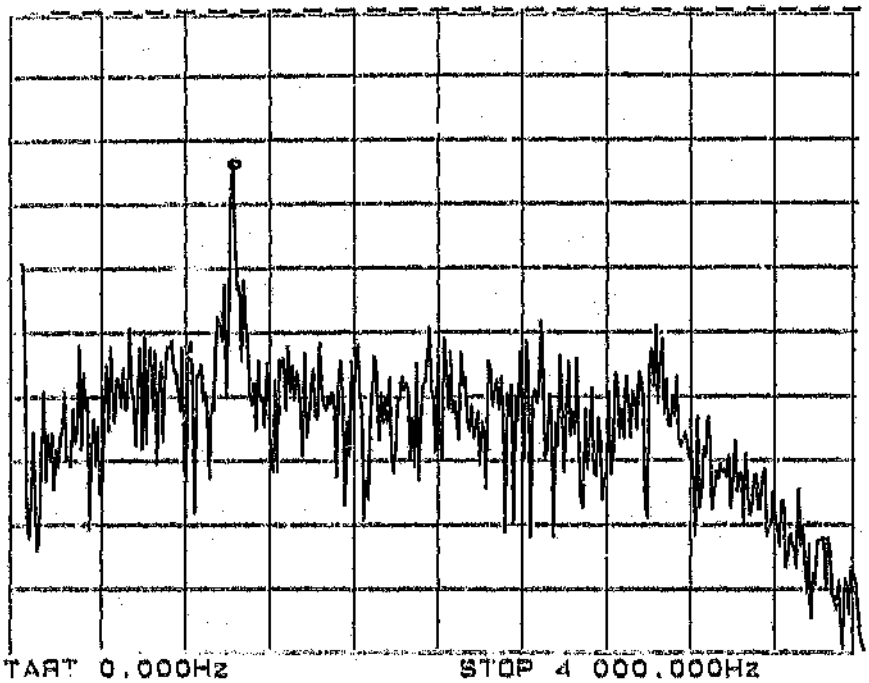
REF LEVEL /DIV MARKER 2 510.000Hz
-5.000dBm 10.000dB MAG (A) -20.827dBm



START 0.000Hz STOP 4 000.000Hz
AMPTD -10.0dBm

FIGURE 28

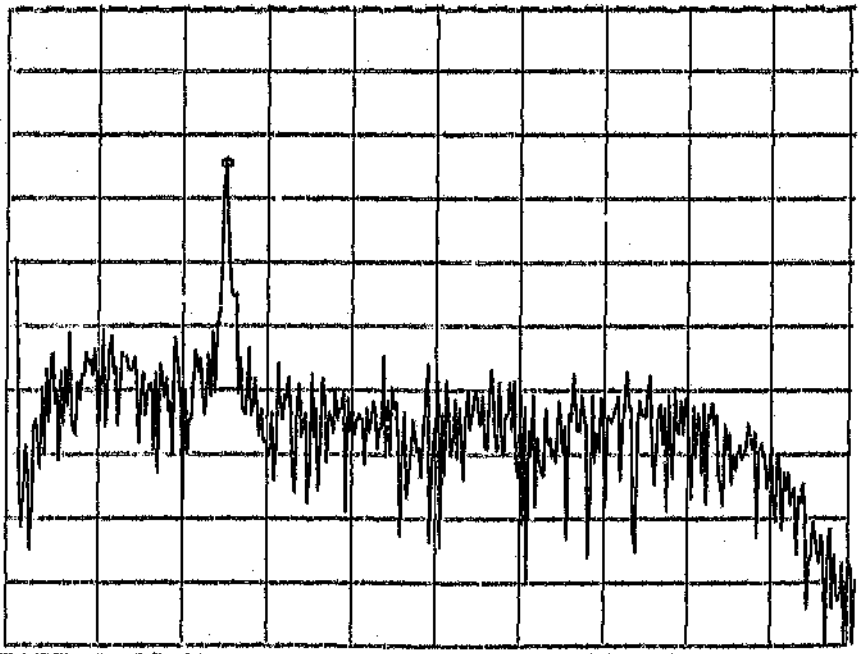
REF LEVEL -5.000dBm /DIV 10.000dB MARKER 1 010.000Hz MAG (A) -28.882dBm



START 0.000Hz STOP 4 000.000Hz
AMPTD -10.0dBm

FIGURE 25

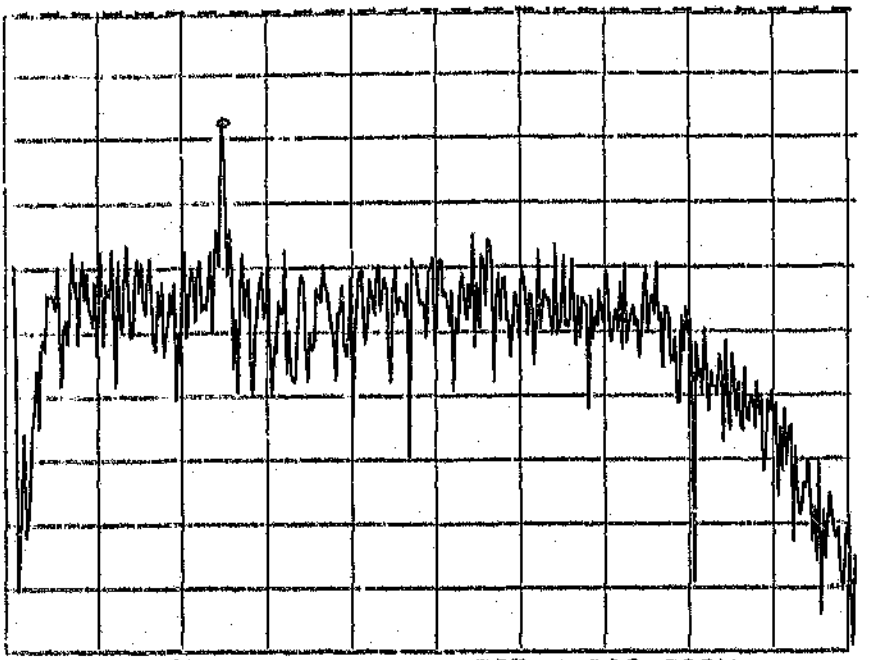
REF LEVEL -5.000dBm /DIV 10.000dB MARKER 1 010.000Hz MAG (A) -29.449dBm



START 0.000Hz STOP 4 000.000Hz
AMPTD -10.0dBm

FIGURE 26

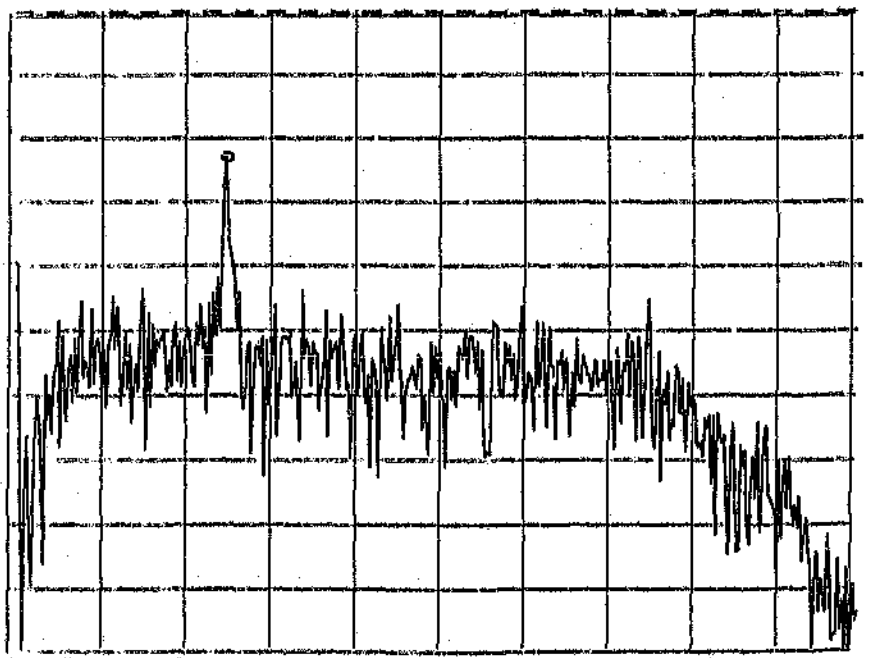
REF LEVEL /DIV MARKER 1 010.000Hz
-5.000dBm 10.000dB MAG (R) -22.356dBm



START 0.000Hz STOP 4 000.000Hz
AMPTD -10.0dBm

FIGURE 23

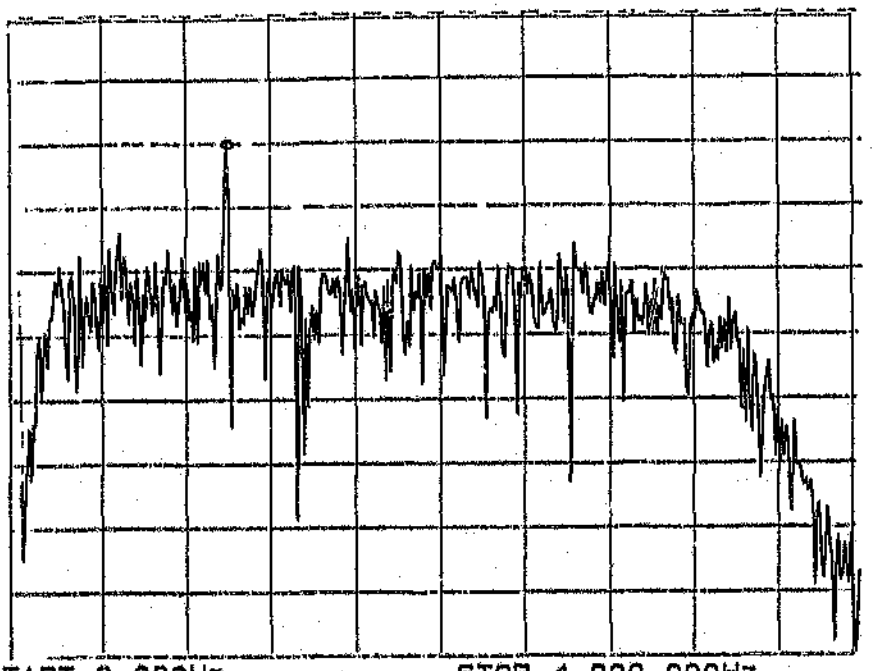
REF LEVEL /DIV MARKER 1 010.000Hz
-5.000dBm 10.000dB MAG (R) -27.789dBm



START 0.000Hz STOP 4 000.000Hz
AMPTD -10.0dBm

FIGURE 24

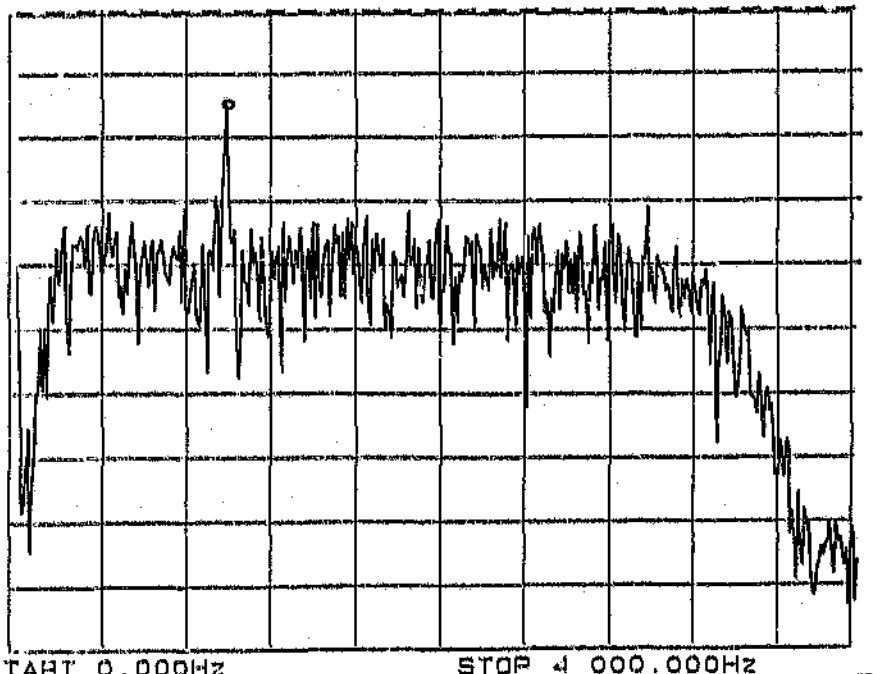
REF LEVEL /DIV MARKER 1 010.000Hz
-5.000dBm 10.000dB MAG (A) -24.944dBm



START 0.000Hz STOP 4 000.000Hz
AMPTD -10.0dBm

FIGURE 21

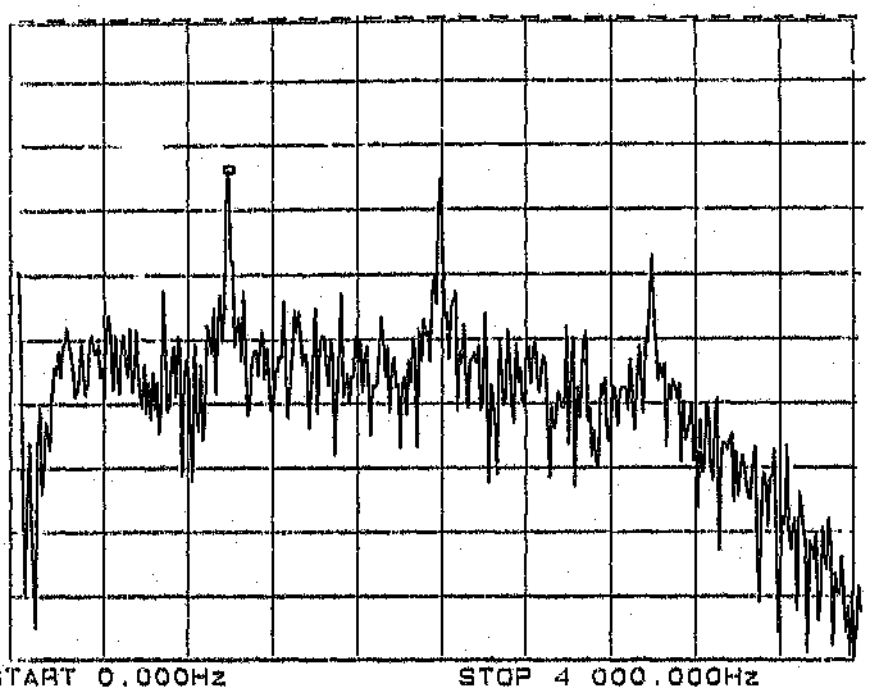
REF LEVEL /DIV MARKER 1 010.000Hz
-5.000dBm 10.000dB MAG (A) -19.615dBm



START 0.000Hz STOP 4 000.000Hz
AMPTD -10.0dBm

FIGURE 22

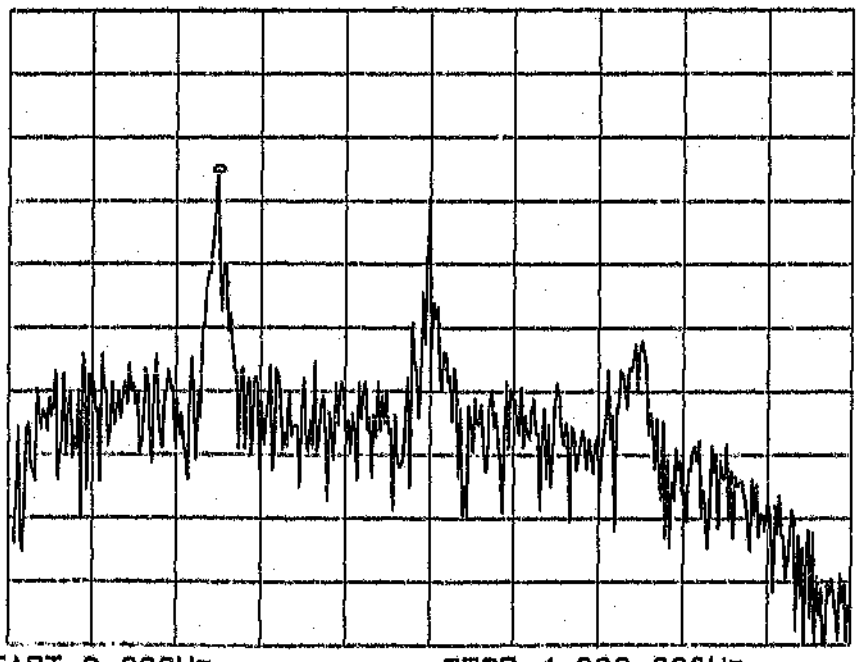
REF LEVEL /DIV MARKER 1 010.000Hz
-5.000dBm 10.000dB MAG (R) -28.545dBm



START 0.000Hz STOP 4 000.000Hz
AMPTD -10.0dBm

FIGURE 19

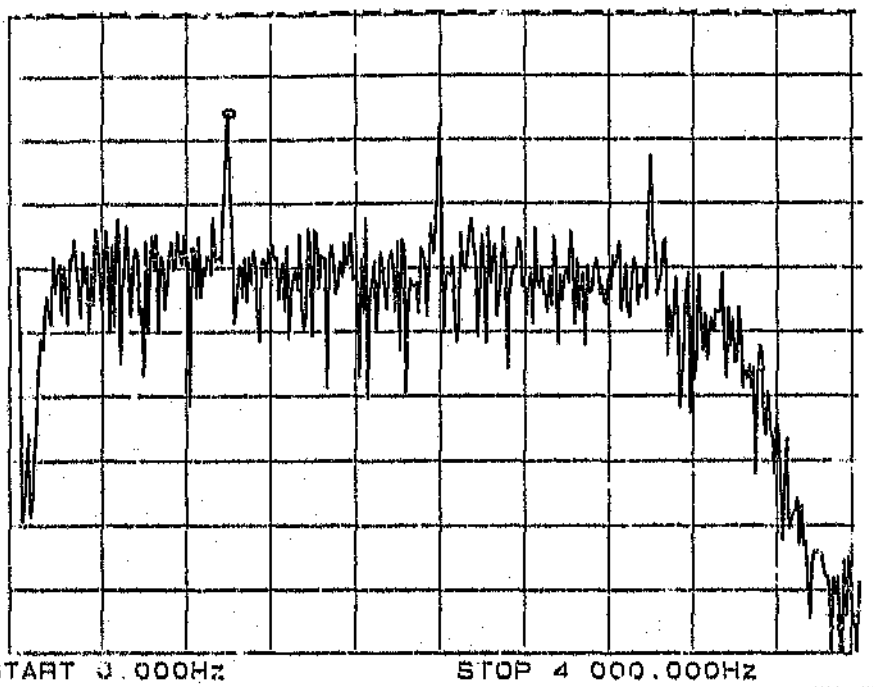
REF LEVEL /DIV MARKER 1 010.000Hz
-5.000dBm 10.000dB MAG (R) -29.904dBm



START 0.000Hz STOP 4 000.000Hz
AMPTD -10.0dBm

FIGURE 20

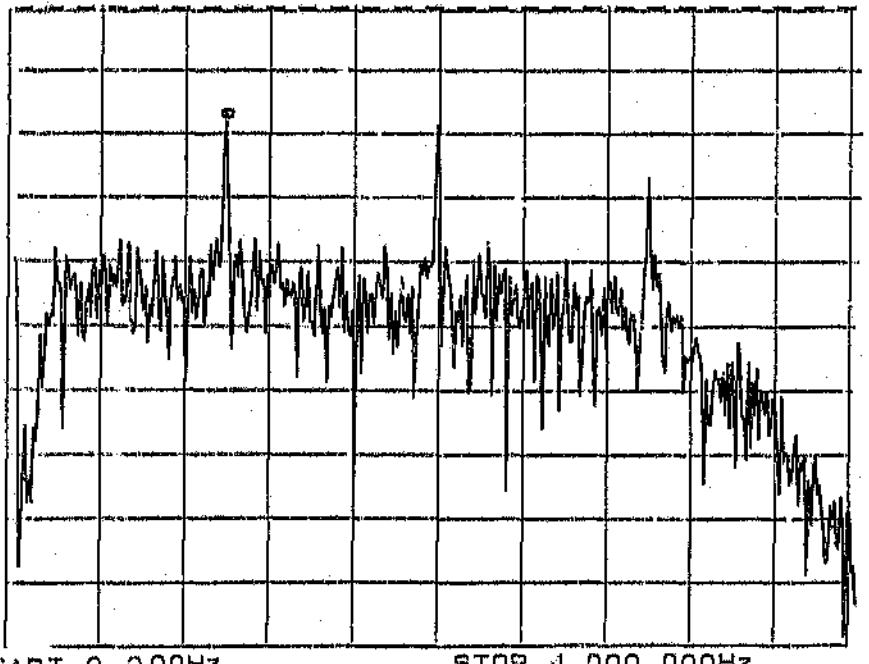
REF LEVEL /DIV MARKER 1 010.000Hz
-5.000dBm 10.000dB MAG (A) -20.516dBm



START 0.000Hz STOP 4 000.000Hz
AMPTD -10.0dBm

FIGURE 17

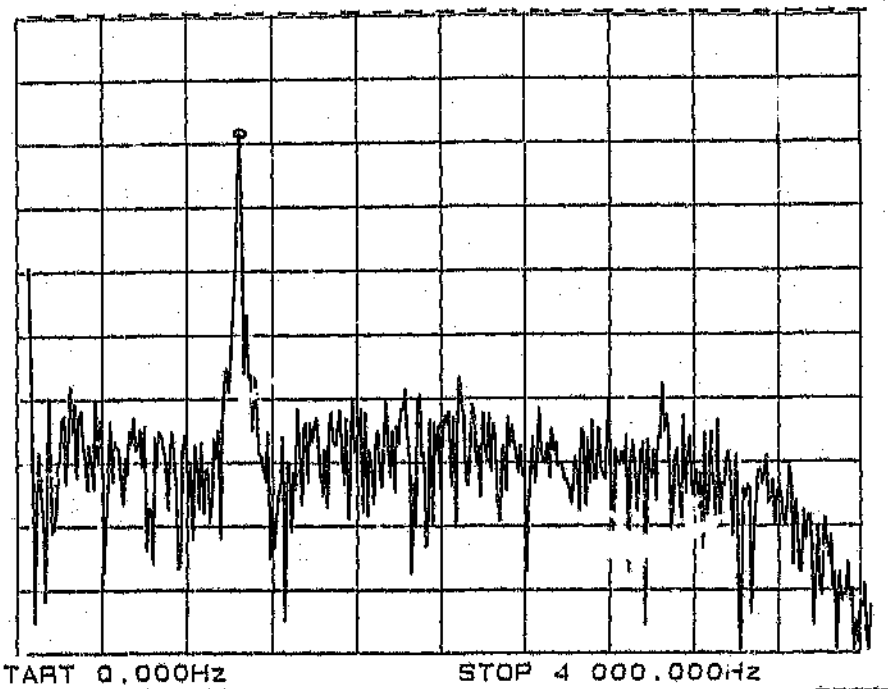
REF LEVEL /DIV MARKER 1 010.000Hz
-5.000dBm 10.000dB MAG (A) -21.503dBm



START 0.000Hz STOP 4 000.000Hz
AMPTD -10.0dBm

FIGURE 18

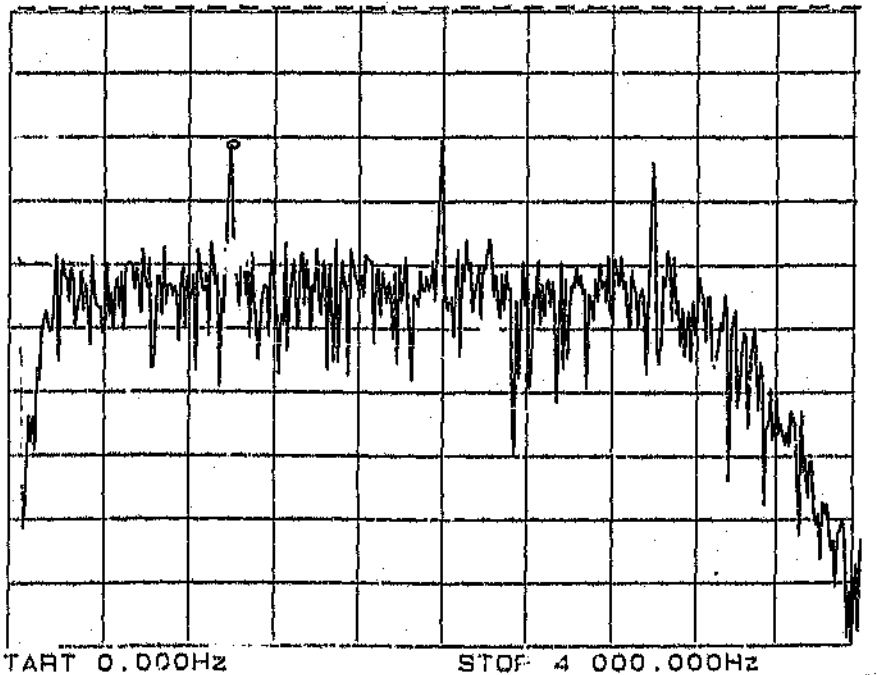
REF LEVEL -5.000dBm /DIV 10.000dB MARKER 1 010.000Hz MAG (A) -23.795dBm



START 0.000Hz STOP 4 000.000Hz
AMPTD -10.0dBm

FIGURE 15

REF LEVEL -5.000dBm /DIV 10.000dB MARKER 1 010.000Hz MAG (A) -26.529dBm



START 0.000Hz STOP 4 000.000Hz
AMPTD -10.0dBm

FIGURE 16

CCIR, (1974) "World Distribution and Characteristics of Atmospheric Radio Noise", Report 322-1, ITU, Geneva.

Craiglow, R.L. (1963) ET AL., "A Study of the Effects of Elementary Processing Techniques on the Intelligibility of Speech in Noise", Collins Radio Res. Rep. CCR 201.

Davenport, W., and Root, W. (1958) : "Random Signals and Noise", McGraw-Hill Book Company, New York.

Dawson, S.L. (1984). Noise Blanker, U.S. Patent 4479251, (Assigned to Rockwell International).

Dutta, S. and Gott, G.F. (1982). HF Spectral Occupancy, IEEE C..e'ence Publication 206 on HF Communication Systems and Techn..ques.

Electronics & Wireless World (September 1989), Reed Business Publishing, U.K., "AM Synchronous Demodulator", p858.

Evans, D.S. and Jessop, G.R. (1976). VHF-UHF Manual, 3rd Edn. RSGB, London, Chapter 2.

Fletcher, H. (1953) "Speech and Hearing in Communications", D. van Nostrand, Princeton, N.J.,

Harris, F.J. (January 1978). "The Use of Windows for Harmonic Analysis", Proc IEEE Vol 66.

REFERENCES

Analog Devices (1989/90), Data Conversion Products Databook. AD1380, 16 bit Sampling ADC.

Bell Telephone Laboratories (1964), Transmission Systems for Communication, Published by Western Electric Company, Tech. Pub., Winston-Salem, N.C.

Best, Dr. Roland E. (1978), "Phase Locked Loops - Theory, Design and Applications, McGraw-Hill Book Company, New York.

Blanchard, A. (1976) "Phase-Locked Loops", Wiley, New York.

Bos and De Boer, Jaes (1966), "Masking and Discrimination", Volume 39, #4.

Brigham, E.O. (1976), "The Fast Fourier Transform and its Application". Englewood Cliffs, NJ, Prentice Hall.

Budden, K.G. (1985) "The Propagation of Radio Waves", Cambridge University Press.

CCIR (1974), "Bandwidth, Signal to Noise Ratio and Fading Allowances in Complete System", Recommendation 339-3, ITU, Geneva.

CCIR, (1978) "Man-Made Radio Noise", Report 258-3, ITU, Geneva.

Test 44 : Local AM station at 576 kHz, with added interference of four frequencies:

573,4 kHz (lower sideband interference of 2,6 kHz)

575,3 kHz (lower sideband interference of 0,7 kHz)

576,5 kHz (upper sideband interference of 0,5 kHz)

577,5 kHz (upper sideband interference of 1,5 kHz)

The switch that activates the sideband selection was switched on and off a few times in order to demonstrate the effectiveness of the circuit.

APPENDIX F : RECORDING

In order to demonstrate the new detector, a recording was made and an audio cassette is attached to this report.

The test was conducted at the Engineering Laboratory of Alcatel Altech Telecoms. The building is made of metal structure with metal roof which acts as a Faraday cage. In addition, due to the large number of p.c.'s and other electronic equipment operating continuously, the background noise level at radio frequencies is high. The recording was done with the microphone placed in front of the speaker. Since the recording level was adjusted to 0 dB, individually for each test, the listener should only refer to the signal to noise ratio and not to the absolute level.

Test 1 to test 41 corresponds to the tests described in Section 4.2.

For reception of radio station an active antenna was used.

Test 42 : The receiver was tuned to 15,615 MHz (Israeli broadcasting) and recorded directly from the ICOM R70 receiver.

Test 43 : The same station as in test 42 as sound from the new detector. Note that at one point the signal to noise ratio was so low that the detector cut the output instead of producing noise as in a normal detector.

The above operations are taking place in IC311 and IC411. IC412 converts the signal into a polar form and the magnitude is passing to IC415 which is a magnitude comparator and to IC413 the look up table for the noise reduction operation. IC414 converts the signal to rectangular form and IC415 selects the correct sideband. IC201 performs off reverse FFT. IC202 converts from floating point to fixed point and IC204 is the D to A converter. IC215 and the associated circuitry act as a compressor in order to compensate for the expending operation of the look up table. IC205 is the audio low pass smoothing filter. IC213 is the audio power amplifier. IC312 is used for control and timing generation.

APPENDIX D : CIRCUIT DESCRIPTION

The IF from the ICOM receiver at frequency of 9,01 MHz is entering to the circuit at LKA1. IC4 converts it to 455 kHz. IC1, IC2 and IC4 are IF amplifiers with AGC control. IC5 multiplies the signal with the 0^0 output from the PLL in order to recover the in-phase components and IC10 is the audio band-pass filter. IC12 is doing the same with the 90^0 output in order to recover the quadrature components and IC13 is the audio band-pass filter. IC14 is PLL1. IC17/C, IC17/D, IC16, IC25 and OSC1 are PLL2. IC6 produces the 90^0 phase shift. IC17/A, IC17/B, IC15, IC32 and IC26 generates AGC output locking on the carrier. IC8 generates wide band AGC that takes over to avoid saturation when the PLL is not locking or when the signal to noise ratio is negative enough to exceed the dynamic range of the system. The in-phase signal is converted in IC401, 16 bit A to D converter to digital form, stored in IC407, IC408 shift register and converted from time domain to frequency domain in IC410, which performs FFT. The quadrature signal has similar pass with IC301, IC307, IC308 and IC310.

The 90^0 phase shift network, which is an essential element in the phasing method for separating the upper and the lower side is not present in this design. Instead the FFT operation itself is utilised. In other words instead of creating a delay in the time domain, the I and the Q components are swopped in the frequency domain. One side band is generated by adding the R of the in-phase to the I of the quadrature, and the I of the in-phase to the R of the quadrature. The other sideband is generated by subtracting the same terms.

The output signal power after the baseband filter is:

$$S_o = A^2\overline{m^2(t)}$$

(App.C-5)

and the noise power after filtering:

$$N_o = 2\eta f_m \qquad \text{(App.C-6)}$$

The signal to noise ratio is:

$$\lambda = \frac{S_0/N_o}{S_i/N_m} = \frac{\overline{m^2(t)}}{1 + \overline{m^2(t)}}$$

(App.C-7)

When the signal to noise ratio is low:

$$\frac{S_o}{N_o} = \frac{\overline{m^2(t)}}{1.1}\left(\frac{S_i}{N_m}\right)^2$$

(App.C-8)

APPENDIX C : ENVELOPE DEMODULATOR

Let the noise be represented by:

$$n(t) = n_c(t)\cos\omega_c t - n_s(t)\sin\omega_c t \qquad \text{(App.C-1)}$$

this is called quadrature component representation because of the appearance in the equation of sinusoids in quadrature.

$n_c(t)$ is the level in the cosine direction and

$n_s(t)$ is the level in the sine direction

The input signal plus noise at the envelop demodulator input is:

$$s_1(t) + n_1(t) = A[1 + m(t)]\cos\omega_c t + n_c(t)\cos\omega_c t - n_s(t)\sin\omega_c t$$

$$= \{A[1 + m(t)] + n_c(t)\}\cos\omega_c t - n_s(t)\sin\omega_c t \qquad \text{(App.C-2)}$$

A = carrier amplitude,

$m(t)$ = arbitrary waveform modulation with level of $|m(t)|<1$

The output signal plus noise before baseband filtering is:

$$s_2(t) + n_2(t)$$

$$= \{(A[1 + m(t) + n_c(t))^2 + n_s^2(t)\}^{1/2}$$

$$= \{A^2[1 + m(t)]^2 + 2A[1 + m(t)]n_c(t) + n_c^2(t) + n_s^2(t)\}^{1/2} \qquad \text{(App.C-3)}$$

If the signal to noise ratio is high then:

$$s_2(t) + n_2(t) \approx \{A^2[1 + m(t)]^2 + 2A[1 + m(t)]n_c(t)\}^{1/2}$$

$$= A[1 + m(t)]\left(1 + \frac{2n_c(t)}{A[1 + m(t)]}\right)^{1/2}$$

$$\approx A[1 + m(t)] + n_c(t) \qquad \text{(App.C-4)}$$

the output signal to noise ratio is:

$$\frac{S_o}{N_o} = \frac{A^4\overline{m^2(t)}}{2\eta f_m A^2 + 3\eta^2 f_m^2}$$

(App.B.8)

since $P_c \equiv A^2/2$, and $N_m \equiv \eta f_m$ we get

$$\frac{S_o}{N_o} = \overline{m^2(t)}\ \frac{P_c}{N_m}\ \frac{1}{1 + \frac{3}{4}(N_m/P_c)}$$

(App.B-9)

APPENDIX B : SQUARE-LAW DEMODULATOR

Assume we have a square-law detector that has $y = kx^2$ in which k is a constant, and signal

$$S_i(t) = A[1 + m(t)] \cos \omega_c t. \qquad \text{(App.B-1)}$$

The input to the demodulator is:

$$x(t) = A[1 + m(t)] \cos \omega_c t + n(t) \qquad \text{(App.B-2)}$$

and the output is

$$y(t) = k(A[1 + m(t)] \cos \omega_c t + n(t))^2 \qquad \text{(App.B-3)}$$

The signal is then passed through bandpass, and the output signal power is:

$$S_o = k^2 A^4 \overline{m^2(t)} \qquad \text{(App.B-4)}$$

the noise power due to the term $2kA_n(t)\cos\omega_c t$ is:

$$N_o' = 4k^2A^2 \frac{\eta}{4} 2f_m = 2k^2A^2 \eta f_m \qquad \text{(App.B-5)}$$

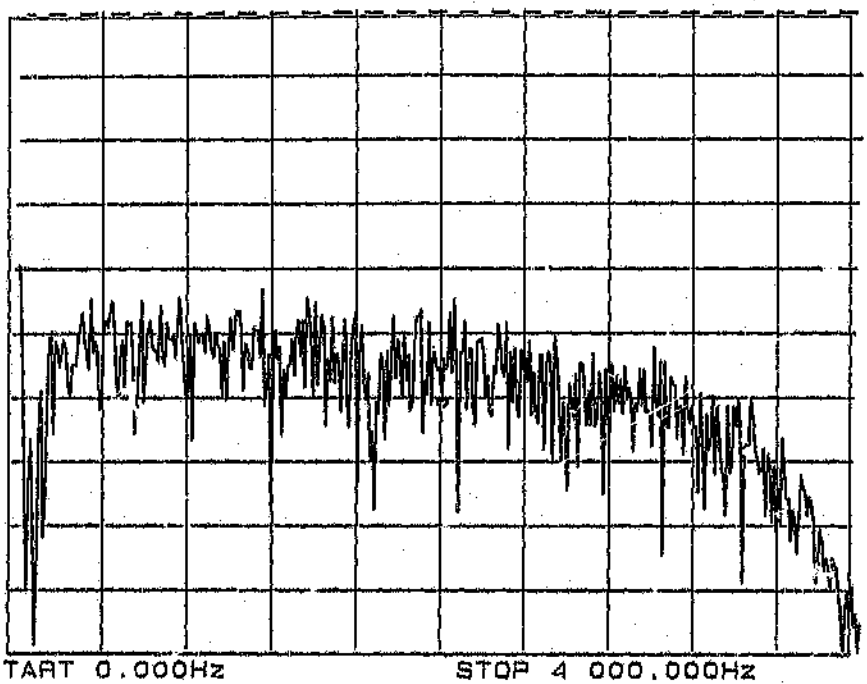
and the noise power due to the term $kn^2(t)$ is :

$$N_o'' = 3k^2 \eta^2 f_m^2 \qquad \text{(App.B-6)}$$

the total output noise power is:

$$N_o = N_o' + N_o'' = 2k^2\eta f_m A^2 + 3k^2\eta^2 f_m^2 \qquad \text{(App.B-7)}$$

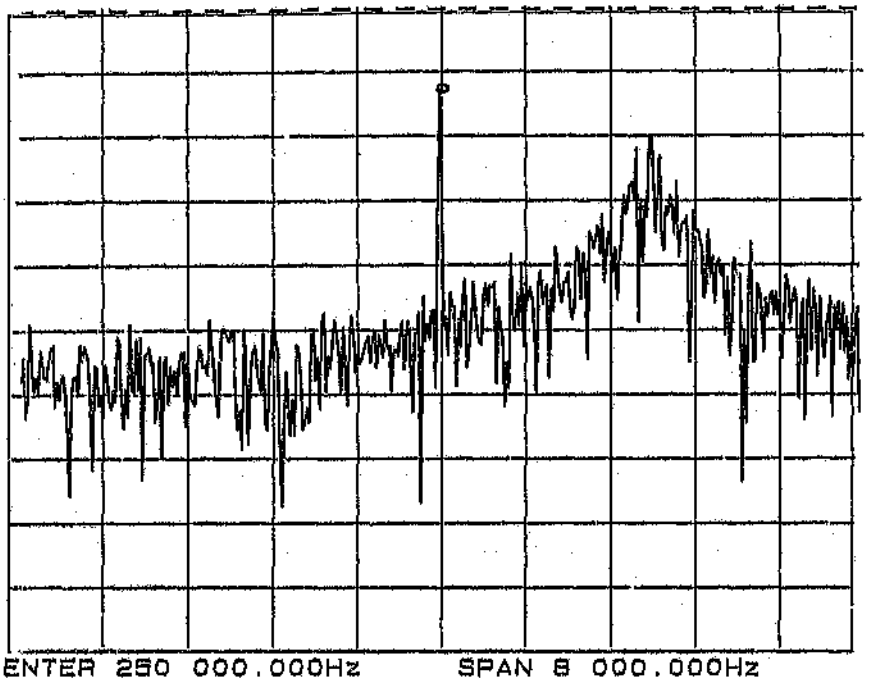
REF LEVEL -5.000dBm /DIV 10.000dB MARKER 2 010.000Hz MAG (A) -65.933dBm



START 0.000Hz STOP 4 000.000Hz
AMPTD -10.0dBm

FIGURE 41

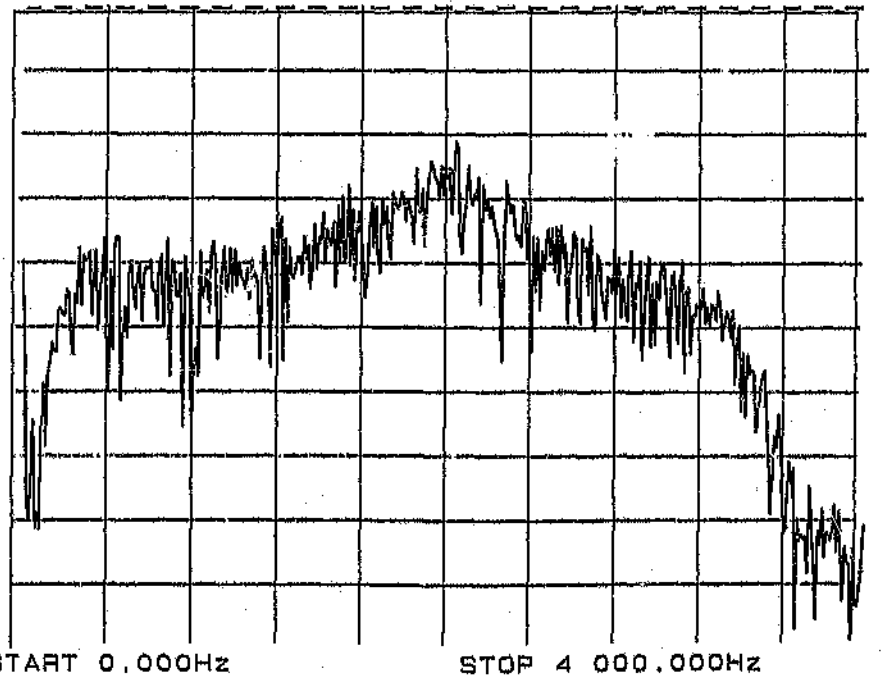
REF LEVEL -40.000dBm /DIV 10.000dB MARKER 250 020.000Hz MAG (A) -52.348dBm



CENTER 250 000.000Hz SPAN 8 000.000Hz
AMPTD -10 0dBm

FIGURE 39

REF LEVEL -5.000dBm /DIV 10.000dB MARKER 2 010.000Hz MAG (A) -30.696dBm



START 0.000Hz STOP 4 000.000Hz
AMPTD -10.0dBm

FIGURE 40

Sheingold, Daniel H., ed. (1986), "Analog-Digital Conversion Handbook", Englewood Cliffs, NJ. Prentice Hall.

Taub, H. and Schilling, D.L. (1971) : "Principles of Communication Systems", McGraw-Hill Book Company, New York.

The American Radio Relay League (1992), "The ARRL Handbook".

Tucker, D.G., (1954) "The History of the Homodyne and Synchrodyne", J. Brit Inst. Radio Engineers, 14, p143.

Viterbi, A.J. (1966), "Principles of Coherent Communications", New York, McGraw-Hill.

Zavrel Jr., R.J. (June 1985). "A Low Power Direct Conversion Side-Band Receiver", ICCE Digest of Technical Papers.

.oOo.

Philips, Linear Products, (1988c), NE/SA572 Programmable Analog Compandor - Product Specification.

Plessey Semiconductors, (1990a). "Digital Signal Processing IC Handbook", PDSP16330.

Plessey Semiconductors, (1990b). "Digital Signal Processing IC Handbook". , PDSP 16340.

Plessey Semiconductors, (1990c). "Digital Signal Processing IC Handbook", PDSP16510.

Radio Society of Great Britain (1982). "Radio Communication Handbook, Fifth Edition".

Roddy, D. and Coolen, J. (1981): "Electronic Communication", Reston Publishing Company, Virginia, p266.

Sabin, William E. and Schoenike, Edgar O. (1987). "Single Sideband System and Circuits", McGraw-Hill Book Company.

Sakrison, D. (1968): "Communication Theory", John Wiley and Sons, Inc., New York.

Shannon, C.E. (January 1949) "Communication in the Presence of Noise, "Proc. IRE, Vol 37, p10-21.

Hawkins and Stevens (1950), "The Masking of Pure Tones and Speech by White Noise", Jaes, Volume 22, #1.

INTEL (1990), Microcommunications Volume 1, 2912A, PCM Transmit/Receive Filter.

Kryter, K.D. (1962) "Methods for the Calculation and use of the Articulation Index", J. Acoust. Soc. AM. Vol 34, p1689-1697.

Law, H.B. (1957). "The Detectability of Fading Radiotelegraph Signals in Noise", Proc. IEE 104B.

Macario, R.C.V., Craine, J.F. and Walters, D.S.,(June 1974) "A Practical Receiver Design for SSB, ISB and AM medium-frequency broadcasts", EBU Technical Review, 145, p101-108.

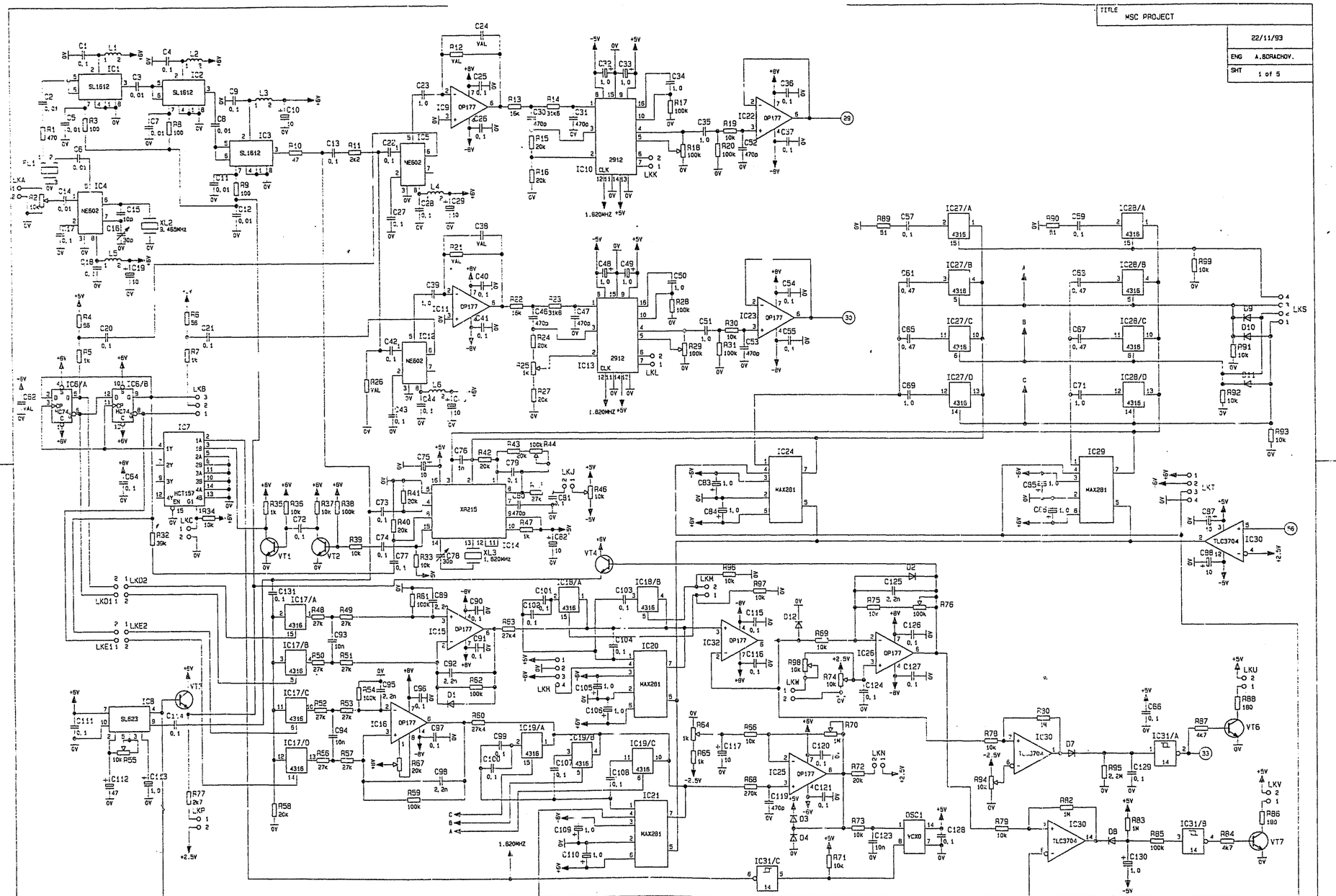
Maslin, N.M., (1987) "HF Communication : A System Approach", Pitman Publishing, p92.

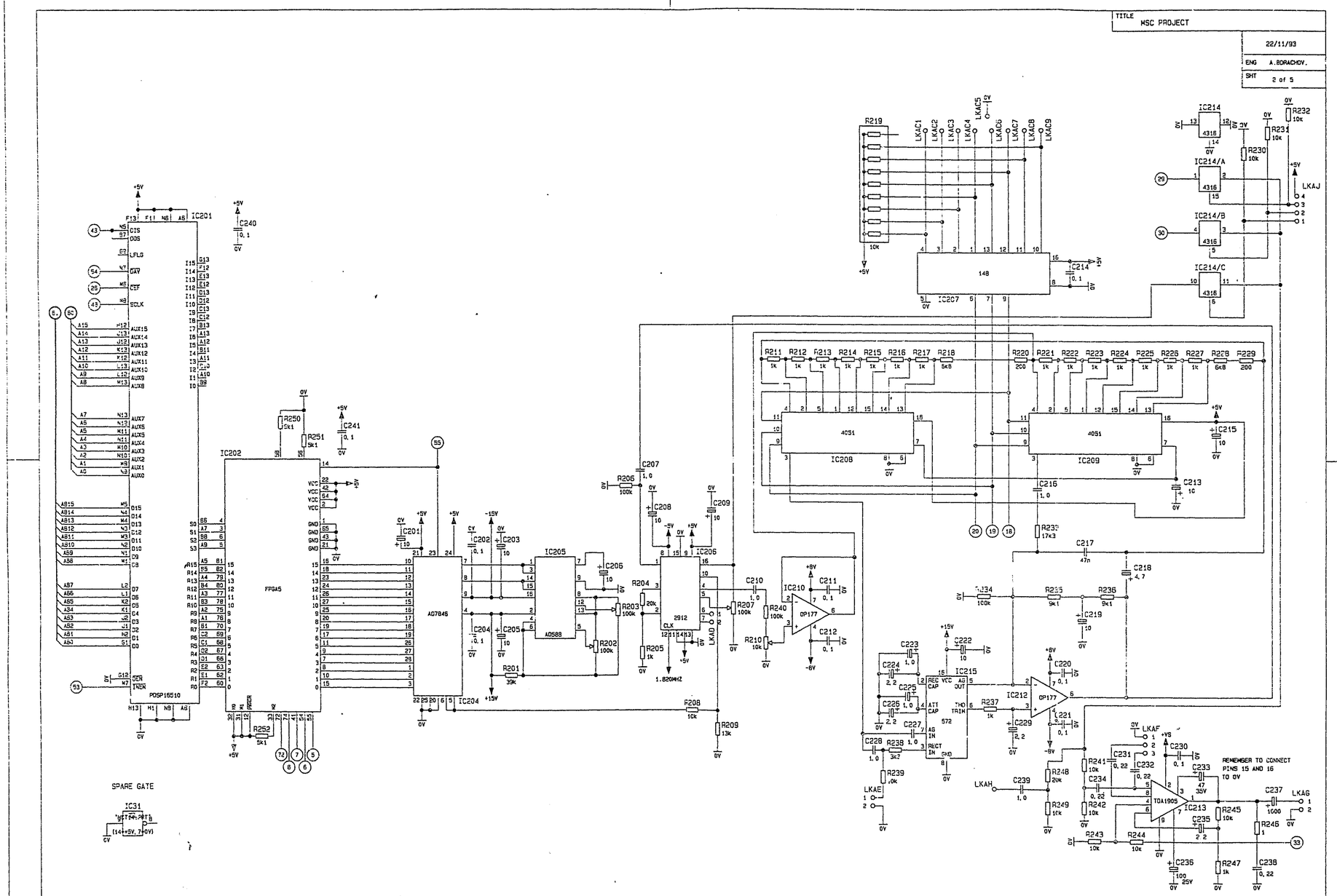
Maslin, N.M. (1987) "HF Communication : A System Approach", Pitman Publishing, p219.

Philips, Linear Products, (1988a). AN198 "Designing with the NE602.

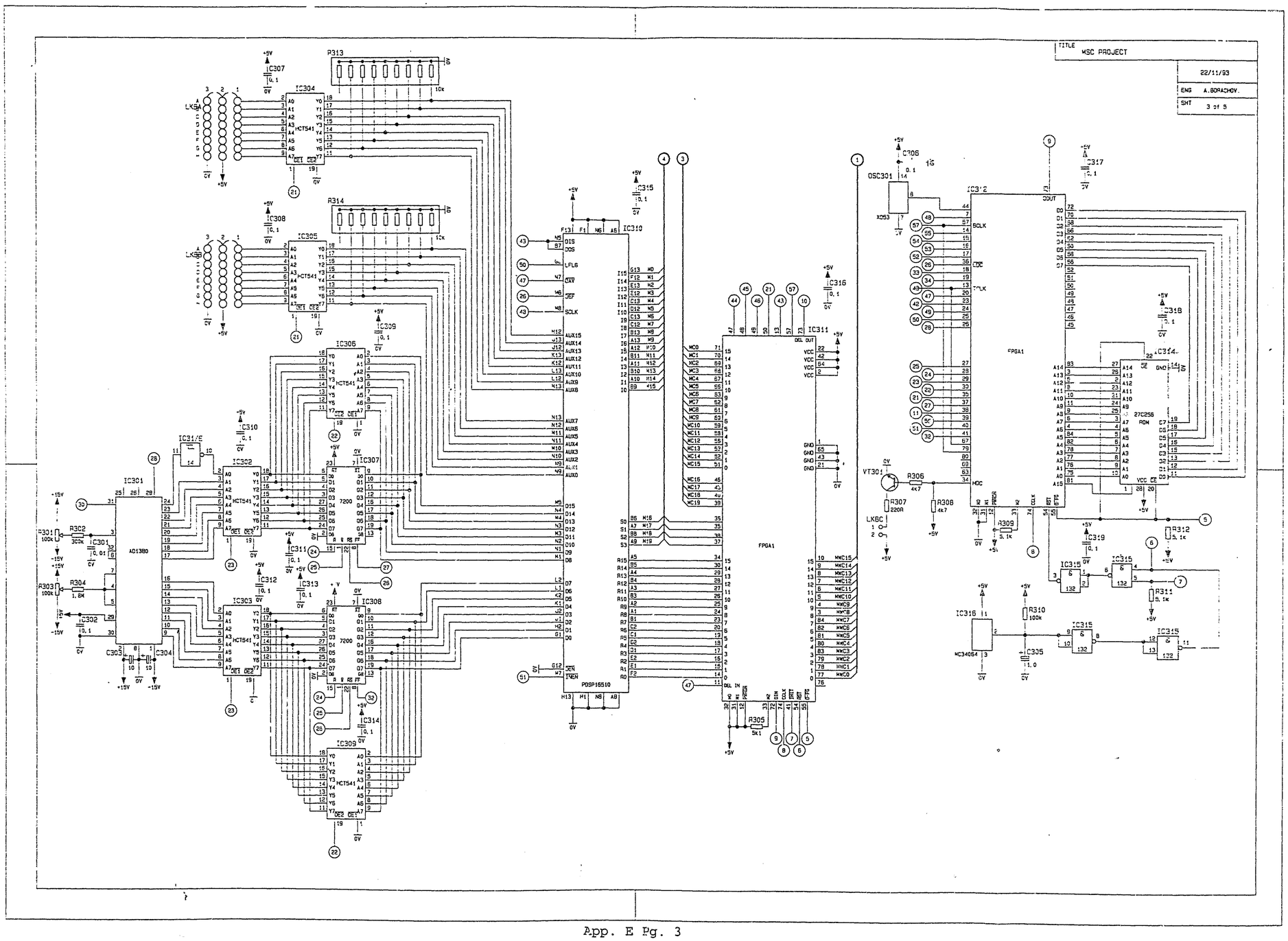
Philips, Linear Products, (1988b), NE/SA602 Double-Balanced Mixer and Oscillator - Product Specification.

APPENDIX E : CIRCUIT DIAGRAM




TITLE
MSC PROJECT
22/11/93
ENG A.BORACHOV.
SHT 2 of 5
IC201
POSP16510
FPGA5
IC202
AD7846
AD588
IC205
IC206
2912
1.820MHZ
IC204
IC207
148
IC208
4051
IC209
4051
IC210
OP177
IC212
OP177
IC214
4316
IC214/A
4316
IC214/B
4316
IC214/C
4316
IC215
REG VCC
CAP
OUT
ATT
CAP
THD
TRIM
AG
IN
RECT
IN
GND
IC232
TDA1905
IC213
SPARE GATE
IC31
REMEMBER TO CONNECT
PINS 15 AND 16
TO 0V
LKAJ
LKAF
LKAE
LKAH
LKAG
LKAD
LKAC1
LKAC2
LKAC3
LKAC4
LKAC5
LKAC6
LKAC7
LKAC8
LKAC9

App. E Pg. 2


TITLE
MSC PROJECT
22/11/93
ENG A.BORACHOV.
SHT 3 of 5
IC307
IC304
IC308
IC305
IC306
IC309
IC302
IC303
IC301
IC310
IC311
IC312
IC313
IC314
IC315
IC316
IC317
IC318
IC319
R313
R314
R301
R302
R303
R304
R306
R307
R308
R309
R310
R311
R312
C301
C302
C303
C304
C305
C306
C307
C308
C309
C310
C311
C312
C313
C314
C315
C316
C317
C318
C319
AD1380
HCT541
7200
FPGA1
P0SP16510
27C256
ROM
OSC301
VT301
MC34064
LK6A
LK6B
LK6C
+5V
-15V
0V

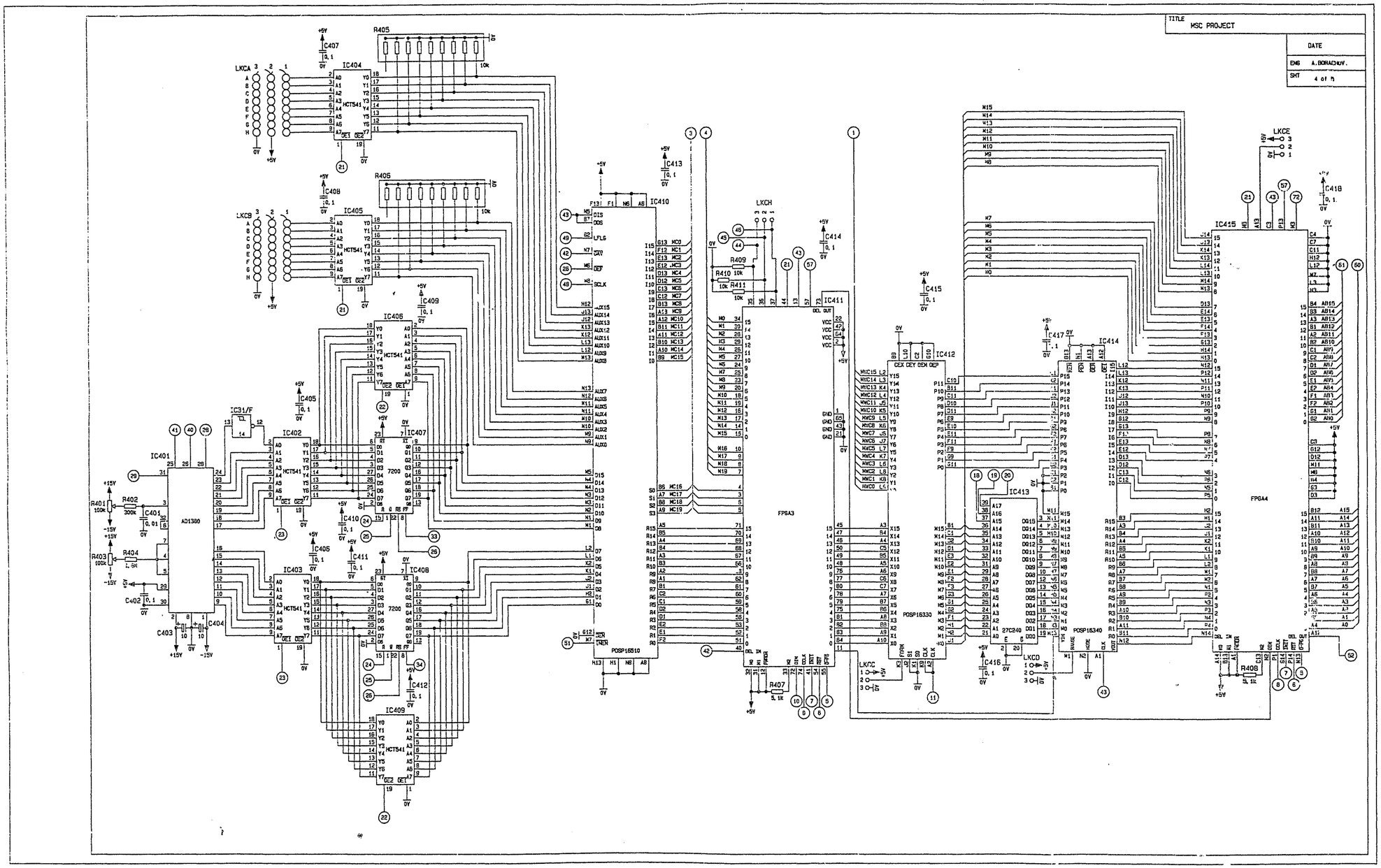
App. E Pg. 3

TITLE
MSC PROJECT

DATE

ENG A.BORACHOV.

SHT 4 of 11

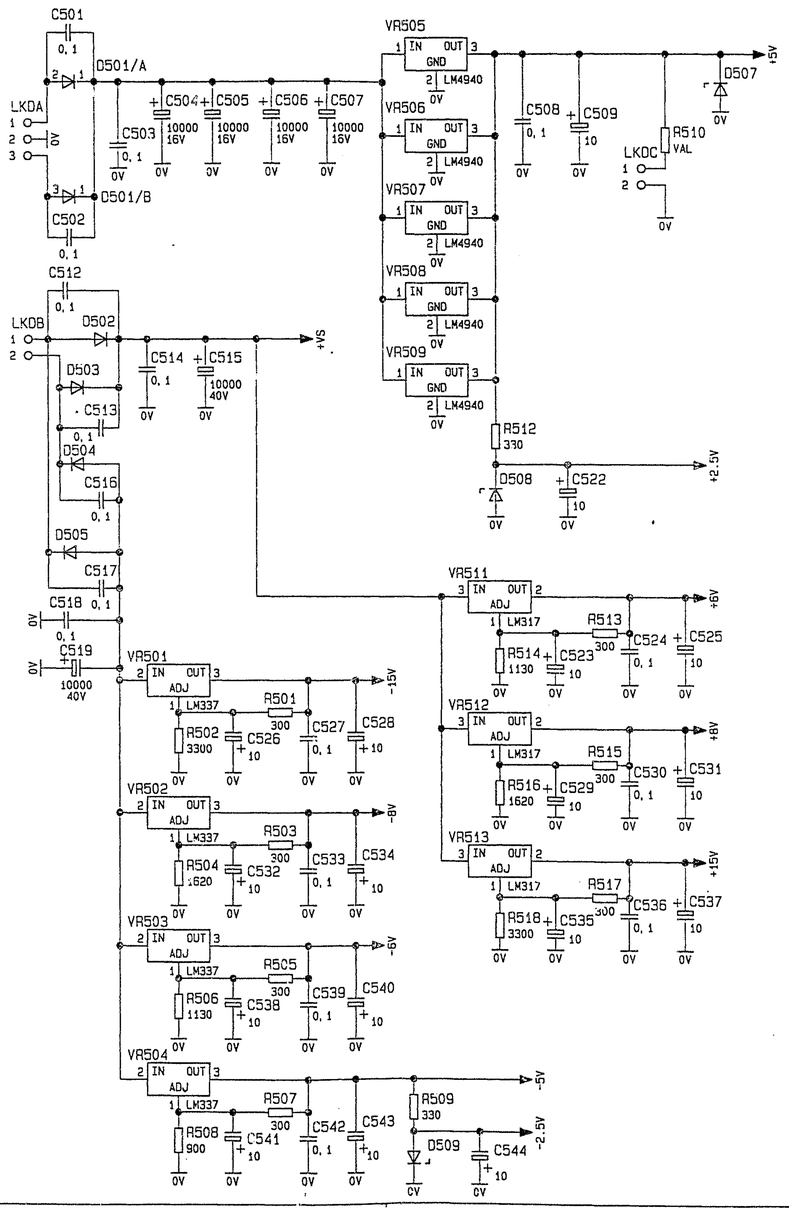


TITLE
MSC PROJECT

4-8-93

ENG A.BORACHOV.

SHT 5 of 5



Author: Borochov Amos.
Name of thesis: Noise and interference reduction in amplitude modulation.

PUBLISHER:
University of the Witwatersrand, Johannesburg
©2015

LEGALNOTICES:

Copyright Notice: All materials on the University of the Witwatersrand, Johannesburg Library website are protected by South African copyright law and may not be distributed, transmitted, displayed or otherwise published in any format, without the prior written permission of the copyright owner.

Disclaimer and Terms of Use: Provided that you maintain all copyright and other notices contained therein, you may download material (one machine readable copy and one print copy per page)for your personal and/or educational non-commercial use only.

The University of the Witwatersrand, Johannesburg, is not responsible for any errors or omissions and excludes any and all liability for any errors in or omissions from the information on the Library website.